TECHNICAL NOTES

NATIONAL ADVISORY COMMITTEE FOR AERONAUTICS

No. 666

LONGITUDINAL STABILITY IN RELATION TO THE USE OF AN AUTOMATIC PILOT

By Alexander Klemin, Perry A. Pepper, and Howard A. Wittner
New York University

Washington
September 1938

NATIONAL ADVISORY COMMITTEE FOR AERONAUTICS

TECHNICAL NOTE NO. 666

LONGITUDINAL STABILITY IN RELATION TO THE USE OF AN AUTOMATIC PILOT

By Alexander Klemin, Perry A. Pepper, and Howard A. Wittner

SUMMARY

The effect of restraint in pitching introduced by an automatic pilot upon the longitudinal stability of an airplane has been studied. Customary simplifying assumptions have been made in setting down the equations of motion and the results of computations based on the simplified equations are presented to show the effect of an automatic pilot installed in an airplane of known dimensions and characteristics. The equations developed have been applied by making calculations for a Clark biplane and a Fairchild 22 monoplane.

INTRODUCTION

Few theoretical studies of the automatic pilot in relation to the longitudinal stability of the airplane have been published to date. A number of interesting questions present themselves, of the following character:

1. What is the effect on the longitudinal dynamic stability of an airplane of the gyroscopic stabilizing element, introduced by the gyroscopic automatic pilot?

2. What modification of the longitudinal static stability is permissible when the gyroscopic stabilizing element is introduced?

3. How is the motion of the airplane in various types of gust affected by the introduction of a gyroscopic stabilizing element?

4. How may the action of an automatic pilot be represented mathematically?

5. What is the effect of a lag in the action of the

automatic pilot, so that the perfect gyroscopic stabilizing element is not available?

6. What is the importance of the fact that, when an airplane runs into a vertical gust, some time passes before the tail surfaces are subjected to the influence of the gust?

An attempt has been made in the present investigation to answer these questions by calculations applied rather fully to the Clark biplane treated in reference 1 and by preliminary calculations applied to the Fairchild 22 airplane.

The equations of motion have been presented in their simplest form, with a number of factors eliminated, to avoid intolerable complexity of calculation and to make the effect of the introduction of the automatic pilot more clearly evident.

I. EQUATIONS OF MOTION WITH A GYROSCOPIC STABILIZING FACTOR

The following equations are based on the system of axes used by the N.A.C.A. and the symbols have their usual significance, except for M_u, M_w, M_q, and M_θ. In this report these symbols are defined as

$$M_u = \frac{\partial M}{\partial u} / m$$

etc., but can be converted to standard form by dividing by k_Y^2.

If all derivatives are referred to unit mass of the airplane and M_u is considered to be zero, the determinantal equation for horizontal motion becomes:

$$\begin{vmatrix} D - X_u & - X_w & g \\ - Z_u & D - Z_w & - U_o D \\ 0 & - M_w & K_B^2 D^2 - M_q D \end{vmatrix} = 0 \qquad (I\text{-}1)$$

If a motion in pitch away from the horizontal introduces a stabilizing factor M_θ, the equation of angular motion becomes

$$K_B^2 \frac{d^2\theta}{dt^2} = M_w w + M_q \frac{d\theta}{dt} + M_\theta \theta$$

so that the determinantal equation is now

$$\begin{vmatrix} D - X_u & - X_w & g \\ - Z_u & D - Z_w & U_o D \\ 0 & - M_w & K_B^2 D^2 - M_q D - M_\theta \end{vmatrix} = 0 \qquad (I-2)$$

Equation (I-1) may be written as

$$A\lambda^4 + B\lambda^3 + C\lambda^2 + D\lambda + E = 0 \qquad (I-3)$$

where

$$A = K_B^2$$

$$B = - (X_u K_B^2 + Z_w K_B^2 + M_q)$$

$$C = X_u M_q + X_u Z_w K_B^2 - X_w Z_u K_B^2 + Z_w M_q - M_w U_o$$

$$D = X_u M_w U_o - X_u Z_w M_q + X_w Z_u M_q$$

$$E = Z_u M_w g$$

Equation (I-2) may be written as

$$A'\lambda^4 + B'\lambda^3 + C'\lambda^2 + D'\lambda + E' = 0 \qquad (I-4)$$

where

$$A' = A$$

$$B' = B$$

$$C' = C - M_\theta$$

$$D' = D + M_\theta(X_u + Z_w)$$

$$E' = E + M_\theta(X_w Z_u - X_u Z_w)$$

Derivatives for the Clark Biplane

Because of the completeness of the information available and because only the general effect of the introduction of the factor $M_{\dot{\alpha}}$ is to be investigated, the Clark biplane of reference 1 has been selected for experimental calculations. The main characteristics and derivatives of this airplane are as follows:

Wing area	464 sq. ft.
Span (maximum)	41 ft.
Stabilizer area	16.1 sq. ft.
Elevator area	16.0 sq. ft.
Tail length	24.5 ft.
Weight	1,805 lb.
Radius of gyration in pitch	4.65 ft.
Air speed	76.9 m.p.h.
U_o	112.5 f.p.s.
Wing setting	0°
X_u	-0.158
X_w	0.356
Z_u	-0.57
Z_w	-5.62
M_u	0
M_w	3.2
M_q	-192.0

When the values of the stability derivatives are inserted in equation (I-3), there is obtained

$$A = 21.62$$

$$B = 316.9204$$

$$C = 1,492.9608$$

$$D = 266.3290$$

$$E = 58.7328$$

so that

$$A' = 21.62$$

$$B' = 316.9204$$

$$C' = 1,492.9608 - M_\theta$$

$$D' = 266.3290 - 5.778\ M_\theta$$

$$E' = 58.7328 - 1.0909\ M_\theta$$

Table I-1 gives the discriminant for various values of M_θ, which, as will be shown later, are attainable with an appropriately geared automatic pilot.

TABLE I-1

Expressions for the Discriminant with Varying Values of M_θ

$M_\theta = 0$	$21.62\lambda^4 + 316.9204\lambda^3 + 1492.9608\lambda^2 + 266.3290\lambda + 58.7328$
$M_\theta = -180$	$21.62\lambda^4 + 316.9204\lambda^3 + 1672.9608\lambda^2 + 1706.3690\lambda + 255.0912$
$M_\theta = -360$	$21.62\lambda^4 + 316.9204\lambda^3 + 1852.9608\lambda^2 + 2346.4090\lambda + 451.4496$
$M_\theta = -720$	$21.62\lambda^4 + 316.9204\lambda^3 + 2212.9608\lambda^2 + 4426.4890\lambda + 844.1664$
$M_\theta = -1080$	$21.62\lambda^4 + 316.9204\lambda^3 + 2572.9608\lambda^2 + 6506.5690\lambda + 1236.8832$
$M_\theta = -2160$	$21.62\lambda^4 + 316.9204\lambda^3 + 3652.9608\lambda^2 + 12746.8090\lambda + 2415.0336$

Variation of Routh's Discriminant with M_θ

For the biquadratic equation

$$A\lambda^4 + B\lambda^3 + C\lambda^2 + D\lambda + E = 0$$

Routh's discriminant, whose magnitude is a rough measure of the stability, is

$$R = BCD - AD - B^2E$$

Routh's discriminant has been calculated for a number of values of M_θ. The results are given in table I-2

TABLE I-2

M_θ	Routh's discriminant
0	118.6×10^6
-180	613.0
-360	1,193.6
-720	2,596.0
-1,080	4,266.1
-2,160	10,960.0

The results of this calculation are also indicated in figure 1. The introduction of M_θ powerfully increases Routh's discriminant.

Variation in Roots with Varying Values of M_θ

Tho roots for varying values of M_θ have been calculated by Graeffe's method, with subsequent improvement in accuracy obtained by E. B. Wilson's method, and the results are given in table I-3. Times to damp to one-half amplitude have also been calculated in the usual manner as well as the periods of oscillation in seconds.

As might be expected on physical grounds, the introduction of M_θ powerfully increases the dynamic stability.

As M_θ increases, the period of the short oscillation decreases, and the damping time lengthens somewhat. The long oscillation passes over into two aperiodic motions, which are powerfully damped.

TABLE I-3

M_θ	Roots	Time to damp to one-half amplitude (sec.)	Period of oscillation (sec.)
0	-7.2410 ± 3.7414i -.0884 ± .1819i	0.0957 7.8410	1.6794 34.5420
-180	-6.8847 ± 4.2085i -0.3160 -.5734	0.1007 2.1935 1.2088	1.4930 - -
-360	-6.5130 ± 4.6320i -0.2337 -1.3989	0.1064 2.9660 .4955	1.3565 - -
-720	-5.8625 ± 5.7536i -0.2127 -2.7209	0.1182 3.2588 .2547	1.0920 - -
-1,080	-5.3480 ± 6.7270i -0.2062 -3.7564	0.1296 3.3615 .1845	0.9340 - -
-2,160	-4.9235 ± 9.8191i -0.2008 -4.6108	0.1408 3.4519 .1503	0.6399 - -

The Order of Magnitude of M_θ

The order of magnitude of M_θ may be conveniently studied from the wind-tunnel tests of the B.E.C.-2 reported in reference 2. This airplane is sufficiently similar to the Clark biplane to serve as a basis for calculation.

For a biplane model of 3.7-foot span, at an air speed of 40 feet per second with elevator neutral, the following pitching moments were obtained:

Angle of attack, α (deg.)	Pitching moment, M (in.-lb.)
0	-0.057
2	-.154
4	-.226

so that

$$\frac{\partial M}{\partial \alpha_{degrees}} = -0.053$$

In the elevator tests, with zero angle of attack, the following values were obtained:

Elevator displacement, δ_e (deg.)	Pitching moment, M (in.-lb.)
0	0.02
5	-.49

so that

$$\frac{\partial M}{\partial \delta_{e_{degrees}}} = -0.094$$

If it is assumed that 1° displacement in pitch would be followed by 3° displacement of the elevator, the ratio

$$\frac{\partial M}{\partial \theta} \Big/ \frac{\partial M}{\partial \alpha} = \frac{3(0.094)}{0.053} = 5.3$$

so that a value of $\partial M/\partial\theta = 6(\partial M/\partial\alpha)$ is a practical possibility.

Since

$$M_w = \frac{1}{U_o}\left(\frac{\partial M}{\partial \alpha}/m\right)$$

$$M_\theta = \left(\frac{\partial M}{\partial \theta} \Big/ \frac{\partial M}{\partial \alpha}\right) U_o M_w$$

$$= \left(\frac{\partial M}{\partial \theta} \Big/ \frac{\partial M}{\partial \alpha}\right) (112.5)\ (-3.2)$$

$$= \left(\frac{\partial M}{\partial \theta} \Big/ \frac{\partial M}{\partial \alpha}\right) (-360)$$

so that M_θ can be calculated for various values of the ratio $\frac{\partial M}{\partial \theta} \Big/ \frac{\partial M}{\partial \alpha}$

$\frac{\partial M}{\partial \theta} / \frac{\partial M}{\partial \alpha}$	M_θ
0.5	-180
1	-360
2	-720
3	-1,080
6	-2,160

II. SIMULTANEOUS VARIATIONS IN THE STATIC STABILITY AND THE GYROSCOPIC STABILIZING FACTOR

Calculations for the Clark Biplane

By obvious manipulations, the constant for the biquadratic of the Clark biplane, at zero angle of attack, can be written in the form

$$A = 21.62$$

$$B = 316.9204$$

$$C = 1,132 - 112.5\ M_w - M_\theta$$

$$D = 209.2 - 17.78\ M_w - 5.778\ M_\theta$$

$$E = -18.50\ M_w - 1.09\ M_\theta$$

In order to obtain a reply to the question "What modification of the longitudinal static stability is permissible when the gyroscopic stabilizing element is introduced?" a number of calculations have been made in which both M_w and M_θ were varied and the results are shown in table II-1. Values of these constants and for Routh's discriminant are given for $M_\theta = 0$, -540, -1.080, and -2,160, with M_w successively given the values 0, -0.8, -1.6, -2.4, -3.2, -4.8, and -6.4. In table II-2 periods and times to damp to one-half amplitude have been calculated for representative combinations; P_1 is the period of the short oscillation and T_1 is the time to damp to one-half amplitude of the short oscillation. Likewise T_{1a} and T_{1b} are the times to damp to one-half amplitude of the two aperiodic motions replacing the short oscillation. For the long os-

cillation, P_2 represents the period and T_2 the time to damp to one-half amplitude. Then T_2 and T_2 are the times to damp to one-half amplitude of the two aperiodic motions replacing the short oscillation. Figure 2 gives a plot of Routh's discriminant for the same representative cases.

From these calculations and charts, it would appear that, once a large value of M_θ has been introduced into the equations of motion, it would be a matter of indifference whether the static stability is double the normal value or reduced to zero.

TABLE II-1

Values of Routh's Discriminant for Changes in M_w and M_θ

M_w	A	B	C	D	E	BCD	AD^2	B^2E	Routh's discriminant
					$M_\theta = 0$				
0	21.62	317	1132	209	0	75.1×10^6	0.94×10^6	0	74.16×10^6
-.8	21.62	317	1222	223	15	87.3	1.08	1.50×10^6	84.72
-1.6	21.62	317	1312	237	30	98.6	1.21	3.02	94.37
-2.4	21.62	317	1402	252	44	112.0	1.38	4.43	106.19
-3.2	21.62	317	1492	266	59	126.8	1.53	5.94	118.33
-4.8	21.62	317	1672	284	89	152.0	1.75	8.96	141.29
-6.4	21.62	317	1852	313	119	184.0	2.13	11.99	169.88
					$M_\theta = -540$				
0	21.62	317	1672	3329	589	17.65×10^8	2.40×10^8	5.92×10^7	14.66×10^8
-.8	21.62	317	1762	3343	604	18.71	2.42	6.06	15.68
-1.6	21.62	317	1852	3357	619	19.70	2.44	6.22	16.64
-2.4	21.62	317	1942	3372	633	20.80	2.47	6.36	17.68
-3.2	21.62	317	2032	3386	648	21.85	2.49	6.51	18.71
-4.8	21.62	317	2212	3414	678	23.93	2.54	6.81	20.71
-6.4	21.62	317	2392	3442	708	26.10	2.58	7.11	22.81

TABLE II-1 - Continued

M_w	A	B	C	D	E	BCD	AD^2	B^2E	Routh's discriminant
					$M_\theta = -1080$				
0	21.62	317	2212	6450	1178	45.23×10^8	8.99×10^8	11.84×10^7	35.06×10^8
-.8	21.62	317	2302	6464	1193	47.17	9.03	11.99	36.94
-1.6	21.62	317	2392	6478	1208	49.12	9.07	12.14	38.84
-2.4	21.62	317	2482	6493	1222	51.09	9.11	12.28	40.65
-3.2	21.62	317	2572	6507	1237	53.05	9.15	12.43	42.66
-4.8	21.62	317	2752	6535	1267	57.01	9.23	12.73	46.51
-6.4	21.62	317	2932	6564	1297	61.15	9.32	13.03	50.53
					$M_\theta = -2160$				
0	21.62	317	3292	12669	2350	132.4×10^8	34.7×10^8	236.1×10^6	95.34×10^8
-.8	21.62	317	3382	12683	2365	136.0	34.8	238.0	98.82
-1.6	21.62	317	3472	12697	2380	139.5	34.9	239.5	102.20
-2.4	21.62	317	3562	12712	2394	143.2	35.0	241.0	105.79
-3.2	21.62	317	3652	12726	2409	147.2	35.2	242.0	109.60
-4.8	21.62	317	3832	12754	2439	155.0	35.3	245.0	117.25
-6.4	21.62	317	4012	12783	2469	163.6	35.4	248.0	125.72

TABLE II-2

Periods P and Times to Damp to One-Half Amplitude, T

M_θ	M_w	P_1 (sec.)	T_1 (sec.)		P_2 (sec.)	T_{2a} (sec.)	T_{2b} (sec.)
-2160	0	0.775	0.188		-	0.097	3.45
	-6.4	.617	.134		-	.165	3.45
-1080	0	1.210	0.176		-	0.104	3.45
	-6.4	.792	.118		-	.246	3.45
-540	0	2.040	0.124		-	0.206	3.45
	-6.4	.938	.106		-	.436	3.48
			T_{1a}	T_{1b}			
0	0	-	0.077	126	-	3.630	-
	-3.2	1.679	0.0957		34.542	7.841	-
	-6.4	1.130	.095	-	26.1	7.680	-

Calculations for the Fairchild 22 Airplane

The calculations made on the Clark biplane in horizontal flight have been repeated for the Fairchild 22 high-wing monoplane, a more modern airplane of somewhat higher loading. In these calculations a horizontal glide, power off, has been considered.

The main characteristics and derivatives of the Fairchild 22 airplane are as follows:

Wing area	171 sq. ft.
Span	32.83 ft.
Stabilizer area	15.8 sq. ft.
Elevator area	10.4 sq. ft.
Tail length	14.69 ft.
Weight	1,600 lb.
Radius of gyration in pitch	4.41 ft.
Air speed	90.7 m.p.h.
U_o	133. f.p.s.
Wing setting	-1°
X_u	-0.0834
X_w	0.2290
Z_u	-0.4830
Z_w	-2.4850
M_u	0
M_w	-2.1300
M_q	-64.0

When these derivatives are inserted in equation (I-1), the expressions for the constants in equation (I-3) become:

$$A = 19.60$$

$$B = 114.40$$

$$C = 170.33 - 133.0\,M_w - M_\theta$$

$$D = 20.38 - 16.57\,M_w - 2.57\,M_\theta$$

$$E = - 15.77\,M_w - 0.318\,M_\theta$$

or

$$A = 19.60$$

$$B = 51.40 - M_q$$

$$C = 6.23 - 2.57\,M_q - 133.00\,M_w - M_\theta$$

$$D = - 0.32\,M_q - 16.57\,M_w - 2.57\,M_\theta$$

$$E = - 15.77\,M_w - 0.318\,M_\theta$$

Effects of variations in M_w and M_θ.- The effects of variations in M_w and M_θ are illustrated in tables II-3 and II-4 and in the curves of figures 3, 4, and 5.

The results of the calculations shown in table II-3 and figure 3 have the same general character as the results of similar calculations for the Clark biplane. As M_θ increases from zero to a value of -270, the long oscillation is replaced by two rapidly damped aperiodic motions. At the same time, the period of the short oscillation becomes more rapid and the time to damp to one-half amplitude lengthens somewhat. The Routh's discriminant increases to relatively enormous values as M_θ increases.

There are very clear lessons to be derived from table II-4 and figures 4 and 5. When M_w is given zero value, the period of the short oscillation becomes unduly long and the long oscillation passes over into two real roots, one of which is zero and the other is of small negative value so that damping is small. But with $M_w = 0$ and even a moderate value of M_θ, the periods and the damping times become satisfactory, and the Routh's discriminant becomes enormous in value. At other values of M_w, it is the value of M_θ that has the predominating effect.

TABLE II-3

Periods and Damping Times for F-22 Airplane; M_w = - 2.13 (original value)

M_θ	Short oscillation		Long oscillation			Routh's discriminant
	Period (sec.)	Times to damp to one-half amplitude (sec.)	Period (sec.)	Times to damp to one-half amplitude (sec.)		
0	1.66	0.241	22.5	12.52	-	2.385×10^6
-270	1.26	.299	-	.673	3.54	49.44
-540	1.03	.337	-	.433	4.40	120.60
-1080	.817	.372	-	.348	4.60	335.06
-2160	.577	.394	-	.314	4.93	1049.57

It would appear that the value of M_w, that is, the magnitude of the static longitudinal stability, is immaterial as long as a gyroscopic stabilizing element can be introduced.

TABLE II-4

Periods and Damping Times for F-22 Airplane

M_θ	M_w	Short oscillation		Long oscillation			Routh's discriminant
		Period (sec.)	Times to damp to one-half amplitude (sec.)	Period (sec.)	Times to damp to one-half amplitude (sec.)		
0	0	14.00	0.241	-	-	5.31	0.388×10^6
	-2.13	1.66	.241	22.50	12.52	-	2.385
	-4.26	1.18	.240	21.00	11.51	-	6.609
-540	0	1.40	0.556	-	0.214	5.52	73.25
	-2.13	1.03	.337	-	.433	4.40	120.60
	-4.26	.863	.303	-	.627	3.63	169.97
-1080	0	0.935	0.465	-	0.251	5.52	242.50
	-2.13	.817	.372	-	.348	4.60	335.06
	-4.26	.714	.336	-	.435	4.36	428.62
-2160	0	0.622	0.441	-	0.268	5.52	866.00
	-2.13	.577	.394	-	.314	4.93	1049.57
	-4.26	.535	.362	-	.368	4.79	1236.14

Effects of variations in M_w and M_q with a constant value of M_θ.- The interesting result that emerges from the calculations shown in table II-5 and in figure 6 is that the Routh's discriminant and the roots of the equations remain satisfactory with a moderate value of M_q even when $M_w = 0$, provided that $M_\theta = -2{,}160$. Only when both M_w and M_q are zero, does instability appear and even then the unstable motion takes 9.85 seconds to double in amplitude.

The preliminary conclusion is that, with the aid of a gyroscopic stabilizing element, both the static stability and the damping moment might be considerably reduced.

Of course, if damping moment were considerably reduced by appreciably shortening the tail arm, there would be difficulty in obtaining high values of M_θ.

Nevertheless, a most interesting prospect of investigation and development appears to lie open, tending to designs in which the length of the fuselage would be considerably shortened. If full advantage were also taken of the possibility of decreasing the moment of inertia about the transverse axis, so that longitudinal restoring or controlling moments could be reduced, there would be an avenue of approach to the tailless flying-wing type of aircraft.

TABLE II-5

Periods and Damping Times for F-22 Airplane

M_θ	M_w	M_q	Short oscillation		Long oscillation		Routh's discriminant
			Period (sec.)	Times to damp to one-half amplitude (sec.)	Period (sec.)	Times to damp to one-half amplitude (sec.)	
-2160	-2.13	-64	0.577	0.394	-	0.314 4.93	1049.57×10^6
		-32	.576	.759	-	.308 4.93	549.11
		0	.574	7.340	-	.308 4.93	76.17
-2160	-1.06	-64	0.601	0.416	-	0.289 5.11	958.8
		-32	.596	.828	-	.288 5.11	483.2
		0	.595	46.000	-	.287 5.11	38.21
-2160	0	-64	0.622	0.441	-	0.268 5.52	866.00
		-32	.617	.927	-	.248 5.65	419.34
		0	.616	[a]9.85	-	.248 5.65	.25

[a]Real part was positive.

III. MOTION IN A SHARP VERTICAL GUST WITH AND WITHOUT THE INTRODUCTION OF A GYROSCOPIC STABILIZING FACTOR

Mathematical Statement

The motion following a sharp upward vertical gust, of magnitude w_o (where w_o is positive), is given by

$$\left.\begin{aligned} (D - X_u)u - X_w w + g\theta &= X_w w_o \\ -Z_u u + (D - Z_w)w - U_o D\theta &= Z_w w_o \\ 0 - M_w w + (K_B^2 D^2 - M_q D)\theta &= M_w w_o \end{aligned}\right\} \quad \text{(III-1)}$$

The equations assume that the line of action of the gust is along the Z axis.

Let

$$\begin{vmatrix} D - X_u & -X_w & g \\ -Z_u & D - Z_w & -U_o D \\ 0 & -M_w & K_B^2 D^2 - M_q D \end{vmatrix} = F(D)$$

The symbolic solutions for the three variables then become:

$$\left.\begin{aligned} u &= w_o \frac{\begin{vmatrix} X_w & -X_w & g \\ Z_w & D - Z_w & -U_o D \\ M_w & -M_w & K_B^2 D^2 - M_q D \end{vmatrix}}{F(D)} \\ w &= w_o \frac{\begin{vmatrix} D - X_u & X_w & g \\ Z_u & Z_w & -U_o D \\ 0 & M_w & K_B^2 D^2 - M_q D \end{vmatrix}}{F(D)} \\ \theta &= w_o \frac{\begin{vmatrix} D - X_u & -X_w & X_w \\ -Z_u & D - Z_w & Z_w \\ 0 & -M_w & M_w \end{vmatrix}}{F(D)} \end{aligned}\right\} \quad \text{(III-2)}$$

The total acceleration along the OZ axis is

$$Dw - U_o D\theta \qquad \text{(III-3)}$$

The actual velocity in space along the OZ axis is given by

$$w_o \frac{\begin{vmatrix} D - X_u & X_w & g \\ -Z_u & Z_w & -U_o D \\ 0 & M_w & K_B^2 D^2 - M_q D \end{vmatrix}}{F(D)} \qquad \text{(III-4)}$$

The actual solutions may be obtained from the modified Heaviside identity

$$\frac{f(D)}{F(D)} = \frac{f(0)}{F(0)} + \sum_{\lambda} \frac{f(\lambda)}{\lambda F'(\lambda)} e^{\lambda t} \qquad \text{(III-5)}$$

whose numerical evaluation has now been dealt with in many publications. (See references 3 and 4.)

When the gyroscopic stabilizing factor M_θ is introduced, the symbolic solutions assume the form:

$$u = w_o \frac{\begin{vmatrix} X_w & -X_w & g \\ Z_w & D - Z_w & -U_o D \\ M_w & -M_w & K_B^2 D^2 - M_q D - M_\theta \end{vmatrix}}{\begin{vmatrix} D - X_u & -X_w & g \\ -Z_u & D - Z_w & -U_o D \\ 0 & -M_w & K_B^2 D^2 - M_q D - M_\theta \end{vmatrix}} \qquad \text{(III-6)}$$

with similar expressions for w and θ.

Solutions of the Equations of Motion

Motion in w.- Solutions of the equations of motion are given in tables III-1, III-2, III-3, III-4, III-5, and III-6.

TABLE III-1

Solutions for w/w_0

M_θ	Constant term	Long oscillation		Short oscillation
0	-1.0000	$-0.0281e^{-0.0884t}\cos(0.1819t - 1.4561)$		$1.0949e^{-7.2410t}\cos(3.7414t - 0.4137)$
		Slowly damped exponential	Rapidly damped exponential	
-180	-1.0000	$-0.0608e^{-0.3160t}$	$0.1055e^{-0.5734t}$	$.9793e^{-6.8847t}\cos(4.2085t - 0.2373)$
-360	-1.0000	$-.0148e^{-0.2337t}$	$.1339e^{-1.3989t}$	$.8898e^{-6.5130t}\cos(4.6320t - 0.0808)$
-720	-1.0000	$-.0110e^{-0.2127t}$	$.3938e^{-2.7209t}$	$.6496e^{-5.8625t}\cos(5.7536t + 0.2599)$
-1080	-1.0000	$-.0075e^{-0.2062t}$	$.6659e^{-3.7564t}$	$.4578e^{-5.3480t}\cos(6.7270t + 0.4092)$
-2160	-1.0000	$-.0079e^{-0.2008t}$	$.8395e^{-4.6108t}$	$.1932e^{-4.9235t}\cos(9.8191t + 0.5076)$

TABLE III-2

Solutions for u/w_0

M_θ	Constant term	Long oscillation		Short oscillation
0	--	$0.3810e^{-0.0884t}\cos(0.1819t - 1.4862)$		$-0.0356e^{-7.2410t}\cos(3.7414t + 0.4258)$
		Slowly damped exponential	Rapidly damped exponential	
-2160	--	$0.0758e^{-0.2006t}$	$-0.0783e^{-4.6108t}$	$0.0033e^{-4.9235t}\cos(9.8191t - 0.7477)$

Table III-1 gives the motion in w (i.e., along the OZ axis) for varying values of M_θ. When the airplane encounters the sharp vertical gust w_o, directed vertically upward or, rather, negatively along the OZ axis, the sum of all the terms evidently represents the actual motion in space. If the constant term is eliminated, the rest of the solution represents the motion relative to the upwardly directed flow of air. As already indicated in section I, the introduction of M_θ splits up the long oscillation into two exponential terms, one slowly damped and the other rapidly damped. Study of table III-1 indicates that, as M_θ is increased progressively:

1. The short oscillation becomes less rapidly damped, but the amplitude of this oscillation diminishes.

2. The slowly damped exponential term becomes progressively less damped, but its amplitude becomes more and more insignificant.

3. The rapidly damped exponential increases in amplitude, but its damping steadily increases.

If the airplane does enter a region where there is a steady vertical motion of air, then the sooner it adjusts itself to this condition and the sooner the "residual" motion disappears, the better. The conclusion is therefore that increasing values of M_θ progressively improve the motion in w.

This conclusion is strengthened by a consideration of the curves of figure 7 where the residual motion in w/w_o is plotted against time; for the extreme cases considered, $M_\theta = 0$ and $M_\theta = -2{,}160$. At $t = 0$, the residual velocity $w/w_o = 1$ in both cases, of course, but the negative values of w/w_o that appear after a second or so are very much smaller in the case of the large value of M_θ and the motion as a whole disappears quite rapidly.

Motion in u.- Results of calculations of the extreme cases for motion in u are tabulated in table III-2. As might be expected on physical grounds, no constant term is present in the solutions of the equations of motion. As in the case of motion in w, the long oscillation splits up into a slowly damped and a rapidly damped exponential

term when the large value of M_θ is introduced. The short oscillation remains but has a considerably shorter period and less damping, just as in the case of motion in w. The value of the constants being so small in all terms, it is clear that the amplitude of the motion in u is greatly reduced by the introduction of the gyroscopic stabilizing factor.

Motion in θ.- The improvement in the pitching moment is still more marked, as indicated by the equations in table III-3 and the curves of figure 8. After a second or so, the motion in θ practically vanishes.

Solution of the Equations of Acceleration along the OZ Axis

From the solutions of the equations of acceleration along the OZ axis, a marked improvement is evident with the resultant acceleration vanishing very rapidly, as is apparent from tables III-4, III-5, and III-6 and from figure 9. There is similarity in the effects produced on w, dw/dt, and U_0q and hence on $(dw/dt) - U_0q$. In all these motions, the short oscillation remains with more rapid period, a trifle slower damping, but lesser amplitude. The long moderately damped oscillation splits up into two exponential terms: one is slowly damped but of very small amplitude; the other is of greater amplitude but very heavily damped. The reason for the improvement is apparent from the solutions for dw/dt and $d\theta/dt$. The values of dw/dt damp out very rapidly, and the values of $d\theta/dt$ are much smaller (as would be expected from the small values of θ). Although the introduction of the gyroscopic stabilizer cannot possibly have an effect on the initial value of the acceleration, which is dependent only on the value of $Z_w w_0$, the virtual disappearance of the pitching motion serves to eliminate the centrifugal forces that subsequently form the larger component of the acceleration.

TABLE III-3

Solutions for θ/w_o

M_θ	Constant term	Long oscillation		Short oscillation
0	—	$-0.0224e^{-0.0884t}\cos(0.1819t - 0.4061)$		$0.0049e^{-7.2410t}\cos(3.7414t - 1.0948)$
		Slowly damped exponential	Rapidly damped exponential	
-2160	--	$0.00001e^{-0.2008t}$	$-0.00150e^{-4.6108t}$	$0.00154e^{-4.9235t}\cos(9.8235t - 0.0283)$

TABLE III-4

Solutions for $\left(\frac{dw}{dt} - U_o q\right)/w_o$

M_θ	Constant term	Long oscillation		Short oscillation
0	—	$-0.0477e^{-0.0884t}\cos(0.1819t - 1.4043)$		$-6.1235e^{-7.2410t}\cos(3.7414t - 0.4117)$
		Slowly damped exponential	Rapidly damped exponential	
-2160	—	$0.0012e^{-0.2008t}$	$-4.6734e^{-4.6108t}$	$-1.0864e^{-4.9235t}\cos(9.8191t + 0.5058)$

TABLE III-5

Solutions for $\frac{dw}{dt}/w_o$

M_θ	Constant term	Long oscillation		Short oscillation
0	--	$-0.0057e^{-0.0884t}\cos(0.1819t - 0.3535)$		$-8.9239e^{-7.2410t}\cos(3.7414t - 0.8907)$
		Slowly damped exponential	Rapidly damped exponential	
-2160	--	$0.0016e^{-0.2008t}$	$-3.8708e^{-4.6108t}$	$-2.1222e^{-4.9235t}\cos(9.8191t - 0.5984)$

TABLE III-6

Solutions for $U_o q/w_o$

M_θ	Constant term	Long oscillation		Short oscillation
0	--	$0.0450e^{-0.0884t}\cos(0.1819t - 1.5133)$		$-4.4888e^{-7.2410t}\sin(3.7414t - 0.0000)$
		Slowly damped exponential	Rapidly damped exponential	
-2160	--	$-0.0003e^{-0.2008t}$	$0.7763e^{-4.6108t}$	$-1.8563e^{-4.9235t}\cos(9.8191t - 1.1317)$

IV. MOTION IN A DELAYED GUST WITH AND WITHOUT THE INTRODUCTION OF A GYROSCOPIC STABILIZING FACTOR

Calculations for motion in a delayed gust of the form $w_o(1 - e^{-t})$ have been carried out for only the two extreme cases, $M_\theta = 0$ and $M_\theta = -2{,}160$. The solutions are presented in tables IV-1 to IV-4 and in the curves of figures 10, 11, and 12. The results show tendencies similar to those present under the action of the sharp gust.

1. With the introduction of a large value of M_θ, the long oscillation again splits up into two exponentials, one slowly damped and one rapidly damped.

2. The motions in w and u are very much better in the constrained airplane.

3. The motion in θ practically disappears on the introduction of M_θ.

4. The maximum acceleration along the OZ axis is slightly smaller when $M_\theta = 0$. Without the introduction of the gyroscopic stabilizing factor, the less constrained airplane ($M_\theta = 0$) has a tendency to head into the resultant wind and to relieve the acceleration. The difference is so slight, however, as to be negligible. Subsequently, the acceleration damps out very much better in the constrained airplane.

TABLE IV-1

Solutions for w/w_o

M_θ	Constant term	Exponential term	Long oscillation		Short oscillation	
0	-1.0000	$1.1449e^{-t}$	$-0.0302e^{-0.0884t}$	$\sin(0.1819t-0.0843)$	$-0.1503e^{-7.2410t}$	$\cos(3.7414t+0.1262)$
			Slowly damped exponential	Rapidly damped exponential		
-2160	-1.0000	$1.2402e^{-t}$	$-0.0099e^{-0.2008t}$	$-0.2325e^{-4.6108t}$	$0.0183e^{-4.9235t}$	$\sin(9.8191t+0.1262)$

TABLE IV-2

Solutions for u/w_o

M_θ	Constant term	Exponential term	Long oscillation		Short oscillation	
0	--	$0.0428e^{-t}$	$-0.3686e^{-0.0884t}$	$\cos(0.1819t+1.4405)$	$0.0047e^{-7.2410t}$	$\cos(3.7414t-0.1470)$
			Slowly damped exponential	Rapidly damped exponential		
-2160	--	$-0.1161e^{-t}$	$0.0948e^{-0.2008t}$	$0.0218e^{-4.6108t}$	$-0.0004e^{-4.9235t}$	$\cos(9.8191t+0.4638)$

TABLE IV-3

Solutions for θ/w_o

M_θ	Constant term	Exponential term	Long oscillation		Short oscillation
0	0.00000	$0.0027e^{-t}$	$-0.0025e^{-0.0884t}\cos(0.1819t-0.5880)$		$-0.0007e^{-7.2410t}\cos(3.7414t-0.4637)$
			Slowly damped exponential	Rapidly damped exponential	
-2160	0.0000	$-0.000386e^{-t}$	$0.000015e^{-0.2008t}$	$0.000429e^{-4.6108t}$	$-0.000429e^{-4.9235t}\cos(9.8191t+1.1593)$

TABLE IV-4

Solutions for $\left(\frac{dw}{dt} - U_o q\right)/w_o$

M_θ	Constant term	Exponential term	Long oscillation		Short oscillation
0	--	$-0.8387e^{-t}$	$0.0414e^{-0.0884t}\cos(0.1819t+1.2513)$		$0.8419e^{-7.2410t}\cos(3.7414t+0.1271)$
			Slowly damped exponential	Rapidly damped exponential	
-2160	--	$-1.2836e^{-t}$	$0.0015e^{-0.2008t}$	$1.2943e^{-4.6108t}$	$-0.1029e^{-4.9235t}\cos(9.8191t-1.4470)$

V. MOTION IN AN INFINITELY SHARP HEAD-ON GUST WITH AND WITHOUT THE INTRODUCTION OF A GYROSCOPIC STABILIZING FACTOR

Calculations have been made for the motion of the same airplane, the Clark biplane, encountering an infinitely sharp head-on gust of strength u_o at $t = 0$.

$$\left.\begin{aligned} (D - X_u)u - X_w w \quad + g\theta &= X_u u_o \\ -Z_u u + (D - Z_w)w - U_o D\,\theta &= Z_u u_o \\ 0 \quad - M_w w \quad + (K_B^2 D^2 - M_q D)\theta &= 0 \end{aligned}\right\} \quad (V\text{-}1)$$

The introduction of the gyroscopic element modifies the pitching-motion equation to

$$0 - M_w w + (K_B^2 D^2 - M_q D - M_\theta)\theta = 0$$

The solutions for the motions in w, u, and θ, and for the acceleration $(dw/dt) - U_o q$ are given in terms of u_o in tables V-1, V-2, V-3, and V-4 and in the curves of figures 13, 14, 15, and 16. In figure 14 the residual motion in u is plotted, that is to say, with the constant term u_o eliminated, because the interest is mainly in knowing how quickly the airplane settles down to its final velocity $U_o - u_o$.

TABLE V-1

Solutions for w/u_o

M_θ	Constant term	Long oscillation		Short oscillation
0	--	$-0.0857e^{-0.0884t}\cos(0.1819t + 0.4296)$		$0.0779e^{-7.2410t}\cos(3.7414t + 0.0727)$
		Slowly damped exponential	Rapidly damped exponential	
-2160	--	$-0.1068e^{-0.2008t}$	$0.1075e^{-4.6108t}$	$-0.0101e^{-4.9235t}\cos(9.8191t - 1.5150)$

TABLE V-2

Solutions for u/u_o

M_θ	Constant term	Long oscillation		Short oscillation
0	-1.00000	$1.11358e^{-0.0884t}\cos(0.1819t+0.4504)$		$-0.00254e^{-7.2410t}\cos(3.7414t+0.9045)$
		Slowly damped exponential	Rapidly damped exponential	
-2160	-1.00000	$1.00955e^{-0.2008t}$	$-0.01002e^{-4.6108t}$	$0.00017e^{-4.9235t}\cos(9.8191t+0.3656)$

TABLE V-3

Solutions for θ/u_o

M_θ	Constant term	Long oscillation		Short oscillation	
0	—	$-0.00712e^{-0.0884t}\cos(0.1819t+1.5299)$		$0.00035e^{-7.2410t}$	$\cos(3.7414t-0.6081)$
		Slowly damped exponential	Rapidly damped exponential		
-2160	—	$0.00016e^{-0.2008t}$	$-0.00020e^{-4.6108t}$	$0.00008e^{-4.9235t}$	$\cos(9.8191t+1.0909)$

TABLE V-4

Solutions for $\left(\frac{dw}{dt} - U_o q\right)/u_o$

M_θ	Constant term	Long oscillation		Short oscillation	
0	—	$-0.15361e^{-0.0884t}\cos(0.1819t+0.5155)$		$-0.43684e^{-7.2410t}$	$\cos(3.74t+0.0703)$
		Slowly damped exponential	Rapidly damped exponential		
-2160	—	$0.02478e^{-0.2008t}$	$-0.59844e^{-4.6108t}$	$0.05680e^{-4.9235t}$	$\cos(9.8191t-1.5130)$

As noted in the previous sections, with the introduction of the gyroscopic stabilizing factor, the long oscillation passes over into two rapidly damped aperiodic motions. The short oscillation has its period lengthened. The amplitudes become very small in all cases. The improvement in the motion due to the introduction of the gyroscopic stabilizing factor is greater than is the case with vertical gusts. This fact is readily explainable by simple physical considerations. In the case of the vertical gusts, in the first instants of the motion, it is a drawback that the gyroscopic stabilizing factor tends to maintain an invariable attitude relative to the horizontal; whereas, without the automatic pilot, the inherent stability tends to vary the angle of attack so as to reduce the accelerating force along the normal axis. But in the case of the head-on gust, the action of the automatic pilot is beneficial from the very first instant, as quite elementary considerations indicate. The incidence of the gust increases the lift and produces an upward motion that decreases the angle of attack. In an ordinary airplane this action would be followed by a positive displacement in pitch. Such a positive displacement is vigorously resisted by the pilot, and hence the normal force and the vertical accelerations are kept down to a minimum. This result is clearly indicated in figure 15. Indirectly all other motions are improved.

VI. MATHEMATICAL REPRESENTATION OF THE ACTION OF THE SPERRY AUTOMATIC PILOT

Simplified Description of the Sperry Automatic Pilot

Reference 5 gives a simplified, yet reliable description of the Sperry Automatic Pilot.

The functioning of this device can be followed by reference to figure 17, which may be taken as applying to the elevator control. The rectangular box indicated in the upper part of the diagram contains the gyroscope and air pick-offs. When the automatic pilot is operating the box is under suction, produced by the suction pump. Air, indicated in figure 17 as entering through the bottom of the box, drives the gyroscope by impinging on buckets on the periphery of the gyroscope rotor. The axis YY' of the gyroscope may be considered as remaining truly vertical

because of a mechanism incorporated in the instrument (but not shown in the diagram), which is designed to correct any precessional movement of the gyroscope.

As shown in figure 18, when the airplane is flying on the desired flight path, both air pick-offs are partly open and pressure is equal on both sides of the air-relay diaphragm. When the airplane pitches, however, the air pick-offs rotate with it, while the gyroscope axis retains its vertical position in space. The relative angular movement between the air pick-offs and the gyroscope causes one pick-off to be more or less completely uncovered while the other pick-off opening is blocked off a like amount. The result of pitching the nose of the airplane up is illustrated diagrammatically in figure 17, where the left pick-off is shown fully open and the right pick-off completely blocked off.

Unequal restrictions are thus imposed on the flow of air entering the air relay through the air inlets on each side of the diaphragm and exhausting into the gyroscope chamber, resulting in a displacement of the diaphragm owing to the unequal pressure drop along the two air paths.

The oil-relay valve, being mechanically connected to the air-relay diaphragm, receives the same displacement as the diaphragm, thereby admitting oil under pressure to the hydraulic servo-cylinder. The servo-cylinder piston, as a result, is displaced to the left. The piston rod, connected to the servo-cylinder piston, protrudes through both ends of the cylinder and, for the case under consideration, would be hooked into the elevator-control system in such a manner that a movement of the piston to the left would deflect the elevator downward.

A speed-control valve Z is used to regulate the speed of response of the piston in accordance with conditions of gustiness. A pressure regulator P prevents the speed of travel of the servo-cylinder piston from exceeding a certain value.

An important element of the gyropilot is the follow-up system. The function of the follow-up is to insure that the control movement will be proportional to the airplane displacement. It is clear that, without the follow-up, any small displacement of the airplane would cause the elevator deflection to continue to increase until it reached the maximum value, unless the airplane in the mean-

time had returned to the preassigned flight attitude. In practice, this characteristic would result in excessive control application, making the airplane overshoot when returning to the desired flight path. Thus any slight disturbance would cause a series of violent, rapidly divergent, oscillations.

The follow-up system consists of a cable and pulley arrangement attached to the servo-cylinder piston rod so that the pulley S (fig. 17) on the gyroscope case is rotated in proportion to the displacement of the servo-cylinder piston. At the other end of the shaft carrying the pulley S is a worm and wheel sector T, which thus rotates the air pick-off assembly in proportion to the displacement of the servo-cylinder piston. When the airplane receives a large disturbance in pitch, considerable displacement of the servo-cylinder piston can occur before the air pick-offs are neutralized by means of the follow-up system and further control displacement is prevented. For small disturbances, however, little control deflection will occur before the follow-up rotates the pick-offs back to neutral.

Information Supplied by the Sperry Gyroscope Corporation

In a communication received from H. Hugh Willis, Research Laboratory of the Sperry Gyroscope Corporation, the following information has been supplied, which is illustrated in figure 19.

> The angular motion of the airplane that occurs before servo control starts varies from 10 to 20 minutes of a degree on commercial Gyropilots. Recently, we have found in the larger airplanes a dead spot of 30 minutes of a degree provided better flying control and we are preloading the balanced oil valve accordingly. For bombing, mapping, etc., we adjust air gaps closer and obtain servo control for angular changes of 6 and 7 minutes of a degree. This causes continued hunting of the control at a frequency approximately 250 cycles a minute. The amount of control is insufficient to affect the attitude of the airplane unless the airplane deviates more than 6 or 7 minutes of a degree.
>
> The speed of servo control varies proportionately with amount of deviation up to 2°. The following curves show the relation of angular change of attitude

of the airplane with regard to the gyro and the resultant servo speed.

The follow-up system limits the amount of control per degree change of attitude of the airplane as follows:

For airplanes sensitive to control, the follow-up ratio is set to permit from 0.25° to 0.8° elevator movement per degree change of attitude. Other airplanes require up to 2° control per degree change of attitude. The average installation uses a 1:1 ratio.

A linear motion of the servo-piston of 1 inch varies angular control motion from 4° to 15°.

Further in actual flying the practice is to restrict servo speed by the servo-speed control valves in the hydraulic system. In smooth air servo speeds are limited to from 1 inch per second to 1 inch per 5 seconds effective on deviations greater than 2°. In turbulent air, speeds are increased up to maximum.

Due to the fact that oil pressures are limited to permit the human pilot overpowering the gyropilot in emergencies there are times in very violent air that control load exceeds servo power and no control occurs momentarily.

Other pertinent information received from the manufacturer is:

1. The limit of the displacement of the elevator by the piston is simply the usual stops on the control cable.

2. On return travel the curve of figure 19 also applies.

3. When the airplane has returned to the same attitude as the gyro, the servo-piston is, of course, at rest.

Discussion of Mathematical Representation

There is reason to believe that the curve of figure 19 is derived from laboratory experiments, while the statements "For airplanes sensitive to control, the follow-up

ratio is set to permit from 0.25° to 0.8° elevator movement per degree change of attitude. Other airplanes require up to 2° control per degree change of attitude." are derived from experience in flight.

To give an exact mathematical representation of the action of the automatic pilot would offer insufferable difficulties, but a qualitative discussion may be of interest and be sufficient for the purposes of this investigation.

Let δ_e, be angular displacement of the elevator.

t_g, time at which the air pick-off has been sufficiently displaced for the automatic pilot to come into play.

Then

$$\delta_e = \int_{t_g}^{t}\int_{t_g}^{t} \ddot{\delta}_e \, dt^2$$

while

$$\theta = \int_{0}^{t}\int_{0}^{t} \ddot{\theta} \, dt^2$$

Also, if R is the pick-off ratio, that is, the ratio by which the displacement of the elevator has to be multiplied in order to give the "backward" travel of the air pick-off and, if θ_g is the lag angle before the pilot comes into play, then the servo-cylinder has a differential pressure acting on it as long as

$$\theta - \theta_g = \int_{0}^{t}\int_{0}^{t} \ddot{\theta} \, dt^2 - \theta_g > R \int_{t_g}^{t}\int_{t_g}^{t} \ddot{\delta}_e \, dt^2$$

when

$$\int_{0}^{t}\int_{0}^{t} \ddot{\theta} \, dt^2 - \theta_g = R \int_{t_g}^{t}\int_{t_g}^{t} \ddot{\delta}_e \, dt^2$$

the servo-cylinder ceases to operate and the elevator, to be displaced.

It is therefore clear that, if R (the pick-off ratio) is always substantially greater than θ, the action of the elevator will be represented substantially by the equation

$$R\,\delta_e = \theta - \theta_g$$

Hence, it follows that the stabilizing action of the automatic pilot can be represented with fair approximation by the term $M_\theta(\theta - \theta_g)$.

From the information given, it would appear that $\ddot{\delta}_e$ is always a constant but, in reality, the automatic pilot provides for adjustment to suit varying atmospheric conditions, with piston acceleration greater under conditions of greater gustiness.

It may also be surmised that the action represented by the equation $R\,\delta_e = \theta - \theta_g$ is assisted by other flight conditions. When a vertical gust, say, first strikes the airplane, the angular acceleration is also at a maximum. After the angular lag has been overcome and before the elevator has been displaced, the acceleration of the servo-cylinder should also be at a maximum. Inasmuch as the angular acceleration of the airplane diminishes under the action of damping and elevator movements, the automatic pilot now encountering a greater hinge moment from the displaced elevator must also impose a lessened acceleration on the elevator.

Further consideration indicates that, when the airplane has received its maximum angular displacement so that $q = 0$, the elevator must also have its maximum displacement. Again, when the airplane begins to return to its normal position, there must again be a lag in the action of the automatic pilot so that its action must now be represented by the expression $M_\theta(\theta + \theta_g)$.

VII. MOTION IN A SHARP VERTICAL GUST WITH LAG IN APPLICATION OF THE GYROSCOPIC STABILIZING FACTOR

The motion in a sharp vertical gust, when there is a lag θ_g in the action of the gyroscopic stabilizing element, can only be determined by a number of calculations of a discontinuous character.

If, at time $t = 0$, the airplane is struck by a sharp upward gust of constant velocity w_o, the equations of motion are those previously given in section III, equation (III-1):

$$\left.\begin{aligned} (D - X_u)u - X_w w \qquad + g\theta \qquad\qquad &= X_w w_o \\ - Z_u u + (D - Z_w)w - U_o D\theta \qquad\qquad &= Z_w w_o \\ 0 \quad - M_w w \qquad + (K_B{}^2 D^2 - M_q D)\theta &= M_w w_o \end{aligned}\right\} \text{(VII-1)}$$

The motion represented by these equations continues until a certain angular displacement θ_g is reached, which is equal to the angular lag of the autonatic pilot. The value of θ_g is determined by the size of the gap in the air pick-off (which is of the order of 7' as a minimum) and the combined or equivalent inertia of the pilot. In these calculations θ_g is assumed to be 0.5°, which probably represents the maximum lag likely to be used for a small airplane.

$$\left.\begin{aligned} (D - X_u)u - X_w w \qquad + g\theta \qquad\qquad &= X_w w_o \\ - Z_u u + (D - Z_w)w - U_o D\theta \qquad\qquad &= Z_w w_o \\ 0 \quad - M_w w \qquad + (K_B{}^2 D^2 - M_q D)\theta &= M_w w_o \\ + M_\theta(\theta - \theta_g) & \end{aligned}\right\} \text{(VII-2)}$$

The calculations for the solutions of equations (VII-2), in view of the calculations previously made in section III, were most conveniently made by splitting up the equations into two parts:

$$\left.\begin{aligned} (D - X_u)u - X_w w \qquad + g\theta \qquad\qquad &= X_w w_o \\ - Z_u u + (D - Z_w)w - U_o D\theta \qquad\qquad &= Z_w w_o \\ 0 \quad - M_w w \qquad + (K_B{}^2 D^2 - M_q D - M_\theta)\theta &= M_w w_o \end{aligned}\right\} \text{(VII-3)}$$

and

$$\left.\begin{aligned} (D - X_u)u - X_w w \qquad + g\theta \qquad\qquad &= 0 \\ - Z_u u + (D - Z_w)w - U_o D\theta \qquad\qquad &= 0 \\ 0 \quad - M_w w \qquad + (K_B{}^2 D^2 - M_q D - M_\theta)\theta &= -M_\theta \theta_g \end{aligned}\right\} \text{(VII-4)}$$

In figure 20, curve A is the solution in θ/w_o of equation (VII-4) and curve B is the solution in θ/w_o obtained by adding the solutions of equations (VII-3) and equations (VII-4) and so obtaining the solution of equations (VII-2). In figure 8, the displacement θ/w_o in radians per foot per second is plotted against time. Assuming a value of 30 feet per second for w_o and putting $\theta_g = 0.5^\circ$, the value of θ/w_o becomes 0.00029. For the motion in which $M_\theta = 0$, this value corresponds to a time $t_g = 0.15$ second, approximately.

After the lag has been overcome, the motion may be represented very closely by equations (VII-2). In these equations the effect of the initial velocities u_g, w_g, and q_g at time $t_g = 0.15$ second is neglected, because they are so small. It is evident that, owing to the lag, the gyroscopic stabilizing factor is indeed represented by the expression $M_\theta(\theta - \theta_g)$, where $\theta_g = 0.5/57.3 = 0.0087$ radian. Here, as in previous sections, $M_\theta = -2,160$.

Of course, the motion represented by curve B of figure 20 or in equation (VII-2) does not continue indefinitely. The motion continues until a maximum displacement in pitch θ_{max} is obtained at which time $q = d\theta/dt = 0$ and $t = t_m = 0.25$ second. (In reality, the actual time at this instant is $t_m + t_g = 0.25 + 0.15 = 0.40$ second.)

At the instant when $q = 0$, the further displacement of the elevator ceases and, on the return displacement of the airplane, the action of the automatic pilot is represented by the expression $M_\theta(\theta + \theta_g)$, owing to the lag. The reversal in lag in these calculations is taken as occurring instantaneously, which is not strictly accurate. To take accurate cognizance of the period of reversal would introduce overwhelming complexities, and no serious errors are introduced by this approximation because θ_g in practice will, for an airplane of the size considered, be considerably smaller than the 0.5° employed in these calculations.

In order to allow for the reversal in lag, the solution of the equations

$$\left.\begin{aligned} (D - X_u)u - X_w w \qquad + g\theta \qquad &= 0 \\ - Z_u u + (D - Z_w)w - U_o D\theta \qquad &= 0 \\ 0 \quad - M_w w \qquad + (K_B^2 D^2 - M_q D - M_\theta)\theta &= 2M_\theta \theta_g \end{aligned}\right\} \text{(VII-5)}$$

is undertaken.

The appropriate values for the solution of equations (VII-5) are plotted in curve C of figure 20.

If curve C is displaced to the right to time t_m = 0.25 second and superimposed on curve B, the resultant motion shown in curve D is obtained. This curve gives apparently a constant value of $\theta/w_o = 0.00025$. But it must be remembered that, in the curves of figure 16, $t = 0$ is, in reality, 0.15 second and that $\theta/w_o = 0$ is, in reality, -0.00029. When appropriate changes are introduced for these initial conditions, the actual motion is that shown in figure 21, in which the fictitious constant value disappears.

Table VII-1 contains a summary of the pertinent solutions. A comparison of the curve of figure 9 with the curve of figure 21 (with M_θ introduced) shows that the lag of the automatic pilot does not change the character of the motion in θ appreciably.

TABLE VII-1

For the equations

$$\begin{aligned} (D - X_u)u - X_w w \qquad + g\theta \qquad &= 0 \\ - Z_u u + (D - Z_w)w - U_o D\theta \qquad &= 0 \\ 0 \quad - M_w w \qquad + (K_B^2 D^2 - M_q D - M_\theta)\theta &= -M_\theta \theta_g \end{aligned}$$

$$\theta/w_o = -0.000256 - 0.000036e^{-0.2008t} + 0.000063e^{-4.6108t} + 0.000269e^{-4.9235t}\cos(9.8191t - 0.3649)$$

$$(D - X_u)u - X_w w + g\theta = 0$$

$$-Z_u u + (D - Z_w)w - U_o D\theta = 0$$

$$0 - M_w w + (K_B^2 D^2 - M_q D - M_\theta)\theta = 2M_\theta \theta_g$$

$$\theta/w_o = 0.000512 + 0.000072e^{-0.2008t} - 0.000126e^{-4.6108t} - 0.000538e^{-4.9235t}\cos(9.8191t - 0.3649)$$

VIII. MOTION IN A VERTICAL GUST WITH INTERVAL OF TIME FOR THE GUST TO REACH THE TAIL SURFACES TAKEN INTO ACCOUNT

When an airplane passes into a region where there is a vertical gust, an interval of time elapses before the vertical gust reaches the tail surfaces. The calculations of this section were made to ascertain the effect of this lag.

Elementary Theory of Gust Lag

If the airplane enters a region in which a steady vertical gust of intensity w_o exists, there is an interval of time $t = l/U_o$ (where l is the distance from the center of pressure of the wing to the center of pressure of the tail surfaces) during which the tail surfaces are not affected by the gust; the angle of attack of the tail surfaces relative to the wing is therefore lessened by an amount w_o/U_o. Thereby a stalling moment is introduced which, referred to unit mass, may be represented by the equation

$$\left.\begin{aligned} M_t &= 57.3 \frac{\rho}{2} U_o^2 S_t \left(\frac{dC_L}{d\alpha}\right)_t \frac{w_o}{U_o} l \frac{1}{m} \\ &= 57.3 \frac{\rho}{2} U_o S_t \left(\frac{dC_L}{d\alpha}\right)_t w_o l \frac{1}{m} \end{aligned}\right\} \quad \text{(VIII-1)}$$

where

ρ, density, 0.002378 slug/cu. ft.

m, mass of airplane, 56 slugs.

S_t, area of horizontal tail surfaces, 32.1 sq. ft.

l, distance between centers of pressure.

$\left(\frac{dC_L}{d\alpha}\right)_t$, slope of lift of tail surfaces, equal to 0.043 per degree. (This low value is due to the low aspect ratio of the tail surfaces, approximately 1.73.)

$w_o = 30$ f.p.s.

so that

$M_t = 127.0$ ft.-lb. per unit mass.

The interval of time $t = l/U_o = 20/112.5 = 0.18$ second.

Motion with Gust Lag Taken into Account Without the Introduction of the Gyroscopic Stabilizing Element

The motion with gust lag taken into account is the sum of the motions represented by the two sets of equations

$$\left.\begin{aligned} (D - X_u)u - X_w w \qquad + g\theta \qquad &= X_w w_o \\ -Z_u u + (D - Z_w)w - U_o D\theta \qquad &= Z_w w_o \\ 0 \quad - M_w w \qquad + (K_B^2 D^2 - M_q D)\theta \; &= M_w w_o \end{aligned}\right\} \quad \text{(VIII-2)}$$

for which solutions have already been obtained in section III, and

$$\left.\begin{aligned} (D - X_u)u - X_w w \qquad + g\theta \qquad &= 0 \\ -Z_u u + (D - Z_w)w - U_o D\theta \qquad &= 0 \\ 0 \quad - M_w w \qquad + (K_B^2 D^2 - M_q D)\theta \; &= M_t \end{aligned}\right\} \quad \text{(VIII-3)}$$

The motion in θ without the vertical gust intervening derived from equations (VIII-3) is given by curve A of figure 22.

The motion in θ due to the gust w_o, obtained from the solution of equations (VIII-2) is given in curve B of figure 22.

The resultant motion due to the gust w_o and to the stalling moment M_t is indicated in curve C of figure 22.

It is interesting to note that, although the vertical gust produces a negative displacement in θ (as might be expected since the statically stable airplane tends to head down into the resultant wind), the stalling moment naturally produces a positive displacement in pitch. The initial disturbance of the airplane in pitch is therefore less marked than when the vertical gust is taken as acting over the entire airplane.

Motion After the Effect of Gust Lag Has Vanished

After the interval of 0.18 second, the vertical gust embraces the entire airplane, and the ensuing motion must be calculated from the equations

$$\left.\begin{aligned}
(D-X_u)u-X_w w \quad & +g\,\theta && = X_w w_o + D u_o' \\
-Z_u u + (D-Z_w)w - U_o D\,\theta \quad & && = Z_w w_o + D w_o' - U_o D\theta_o' \\
0 \quad -M_w w \quad & +(K_B^2 D^2 - M_q D)\theta && = M_w w_o + K_B^2 D^2 \theta_o' - M_q D\theta_o' \\
& && \quad + K_B^2 D q_o'
\end{aligned}\right\} \text{(VIII-4)}$$

where

u_o', is the velocity along the OX axis at $t = 0.18$ and $u_o'/w_o = 0.0330$.

w_o', velocity along the OZ axis at $t = 0.18$ and $w_o'/w_o = -0.5720$.

θ_o', angular displacement in pitch at $t = 0.18$ and $\theta_o'/w_o = 0.00025$.

q_o', pitching angular velocity at $t = 0.18$ and $q_o'/w_o = 0.0057$.

The calculation is continued by introducing u_o', w_o', θ_o', and q_o' as initial values.

In order to solve equations (VIII-4), it is convenient to separate them into the equations

$$\begin{aligned}(D - X_u)u - X_w w \qquad + g\,\theta \qquad &= X_w w_o \\ - Z_u u + (D - Z_w)w - U_o D\,\theta \qquad &= Z_w w_o \\ 0 \quad - M_w w + (K_B^2 D^2 - M_q D)\theta &= M_w w_o\end{aligned}$$

for which solutions are already available from section III and the following equations, which allow for the initial conditions:

$$\left.\begin{aligned}(D-X_u)u-X_w w \quad +g\,\theta \qquad &= Du_o' \\ -Z_u u +(D-Z_w)w-U_o D\,\theta \qquad &= Dw_o' \quad -U_o D\theta_o' \\ 0 \quad -M_w w \quad +(K_B^2 D^2 -M_q D)\theta &= K_B^2 D^2 \theta_o' - M_q D\theta_o' \\ &\qquad\qquad +K_B^2 Dq_o'\end{aligned}\right\} \qquad \text{(VIII-5)}$$

The solution in θ from equations (VIII-5) is

$$\theta/w_o = - 0.00256e^{-7.241t}\cos(3.7414t - 0.8185)$$

$$+ 0.00234e^{-0.0884t}\cos(0.1819t-0.5441) \qquad \text{(VIII-6)}$$

The complete motion, including that indicated in curve C of figure 22 and the subsequent motion obtained by the solution of equation (VIII-4), is shown in figure 23. The curve has been plotted only up to the time $t = 3.0$ seconds from the initial instant when the vertical gust first struck the airplane.

It is interesting to compare the motion in θ of figure 19 with that indicated in figure 8. When the upward vertical gust is taken as striking the entire airplane instantaneously, the maximum angular disturbance is a negative one. When the delay in reaching the tail surfaces is taken into account, the maximum angular disturbance is a positive one, although it is much smaller numerically than when the delay is neglected.

From this result, it is inferred that:

1. The vertical acceleration is certain to be greater when the gust lag is taken into account, because the angle of attack of the main wings is actually increased by the action of the gust.

2. It has been sufficiently demonstrated by previous sections that the action of the gyroscopic stabilizing element is always to reduce the angular disturbance. Because there is a greater angular disturbance with this type of gust lag, the automatic stabilizer should be even more valuable under such circumstances.

CONCLUSIONS

Owing to the complexity of the subject, the present investigation can only be regarded as a preliminary one. Also the investigation suffers from the fact that calculations have been restricted substantially to one airplane. Nevertheless, a method of approach has been established, and certain tentative conclusions may be set down.

1. The introduction of a gyroscopic stabilizing element is, in general, a most powerful method of increasing the stability of an airplane.

2. The introduction of a gyroscopic stabilizing element has a slightly detrimental effect on the short oscillation, whose period becomes more rapid and whose damping time increases. In an ultrasimplified conception of the short oscillation, velocity along the X axis may be considered to remain constant. With this assumption the airplane may be imagined as running into a region in which a vertical upward current exists. Immediately the airplane tends to rise owing to the increased angle of attack but tends at the same time to nose down into the relative wind. Also, as the airplane tends to rise, the relative angle of attack again diminishes. Therefore the initial excess of lift does not exist very long, and the motion is rapidly damped. When, however, the gyroscopic stabilizing element is introduced, it tends to oppose the nosing down into the relative wind, so that the initial excess lift is somewhat greater than with the naturally stable airplane. This explanation gives in rough and simplified fashion the detrimental effect on the short oscillation. At the same time every calculation presented in this report indicates that the effect of the gyroscopic stabilizing element on the short oscillation is not serious.

3. The long oscillation may be very roughly considered in the light of Lanchester's treatment of the phugoid. The airplane of natural inherent stability is supposed to nose down immediately into the relative wind and hence to have no excess lift. It therefore moves downward acquiring excess velocity and excess lift, until the excess lift gives it an upward velocity in excess of the upward velocity of the gust. But this motion takes an appreciable time; and the oscillation therefore has a slow period and slow damping. When, however, the gyroscopic stabilizing element is introduced, the travel along a downwardly inclined path is soon checked, the attitude to the horizontal remains almost unchanged, and the excess lift soon disappears; the airplane assumes the steady motion of the upward current of air, with rapid disappearance of the disturbance. This discussion is oversimplified but explains the replacement of the long oscillation by two well-damped aperiodic motions, as always indicated in the calculations of this report.

4. When the coefficients C, D, E of the biquadratic equation are studied in detail, it is seen that the effect of the introduction of M_θ overshadows the effect of M_w. It may almost be said that it is immaterial what the value of M_w may be, provided that a realizable value of M_θ is introduced into the airplane.

5. When, as for the Fairchild 22 airplane, the values of M_q are varied, it is seen that M_θ again overshadows the effect of M_q and, with considerably reduced values of M_q, it is again possible to secure satisfactory values of periods and damping times by the use of M_θ.

6. Even when M_w and M_q are simultaneously reduced, M_θ proves a cure-all.

7. It follows therefore that, if an adequate gyroscopic stabilizing element is introduced, the airplane designer need have much less worry regarding longitudibal static stability or damping. Interesting departures from classical airplane design are thus in prospect with the use of the automatic pilot. Of course, conservative airplane designers will not at once abandon their efforts to secure inherent longitudinal stability; nevertheless, their thoughts ought well be turned in this direction

8. When the actual motion of the airplane is studied with the introduction of the gyroscopic stabilizing element, it is seen that the improvement in motion might be predicted from the study of the biquadratic equation and its roots. Such an improvement is found to occur in every type of disturbance studied; sudden vertical gust, delayed vertical gust, sudden head-on gust. It is in the decreased amplitude of the pitching motion that the improvement is most marked; again, when encountering the head-on gust, the improvement in the motion is even more marked than in encountering the vertical gusts.

9. The mathematical representation of the action of the automatic pilot is far from complete. Nevertheless, it should be a close approximation to actual conditions. When the lag of the automatic pilot is taken into account, with a magnitude greater than that likely to occur in practice for an airplane of the size considered in this report, there is a lesser improvement than when the "ideal" gyroscopic stabilizing element is introduced. The character of the improvement in motion remains substantially the same and, provided that the designers of the automatic pilot keep lag within close limits and prevent hunting within the unit itself, it is fair to think of the automatic pilot as being close to the action of the "ideal" gravitational stabilizer.

10. The effect of delay of a vertical gust in reaching the tail surface is shown to be relatively unimportant and not likely to affect the general conclusions.

11. There is ample room for further investigation of the subject, which the tremendous potentialities of the automatic pilot would fully justify.

Daniel Guggenheim School of Aeronautics,
New York University,
New York, N.Y., June 1938.

REFERENCES

1. Hunsaker, Jerome: Dynamical Stability of Aeroplanes. Smithsonian Miscellaneous Collections, vol. 62, no. 5, 1916.

2. Bairstow, Leonard: Applied Aerodynamics. Longmans, Green and Co. (London), 1920, pp. 184 and 199.

3. Klemin, Alexander, and Ruffner, Benjamen F.: Operator Solutions in Airplane Dynamics. Jour. Aero. Sci., vol. 3, no. 7, May 1936, pp. 252-255.

4. Jones, Robert T.: A Simplified Application of the Method of Operators to the Calculation of Disturbed Motions of an Airplane. T.R. No. 560, N.A.C.A., 1936.

5. Bassett, Preston R.: Development and Principles of the Gyropilot. Instruments, vol. 9, no. 9, September 1936, pp. 251-254.

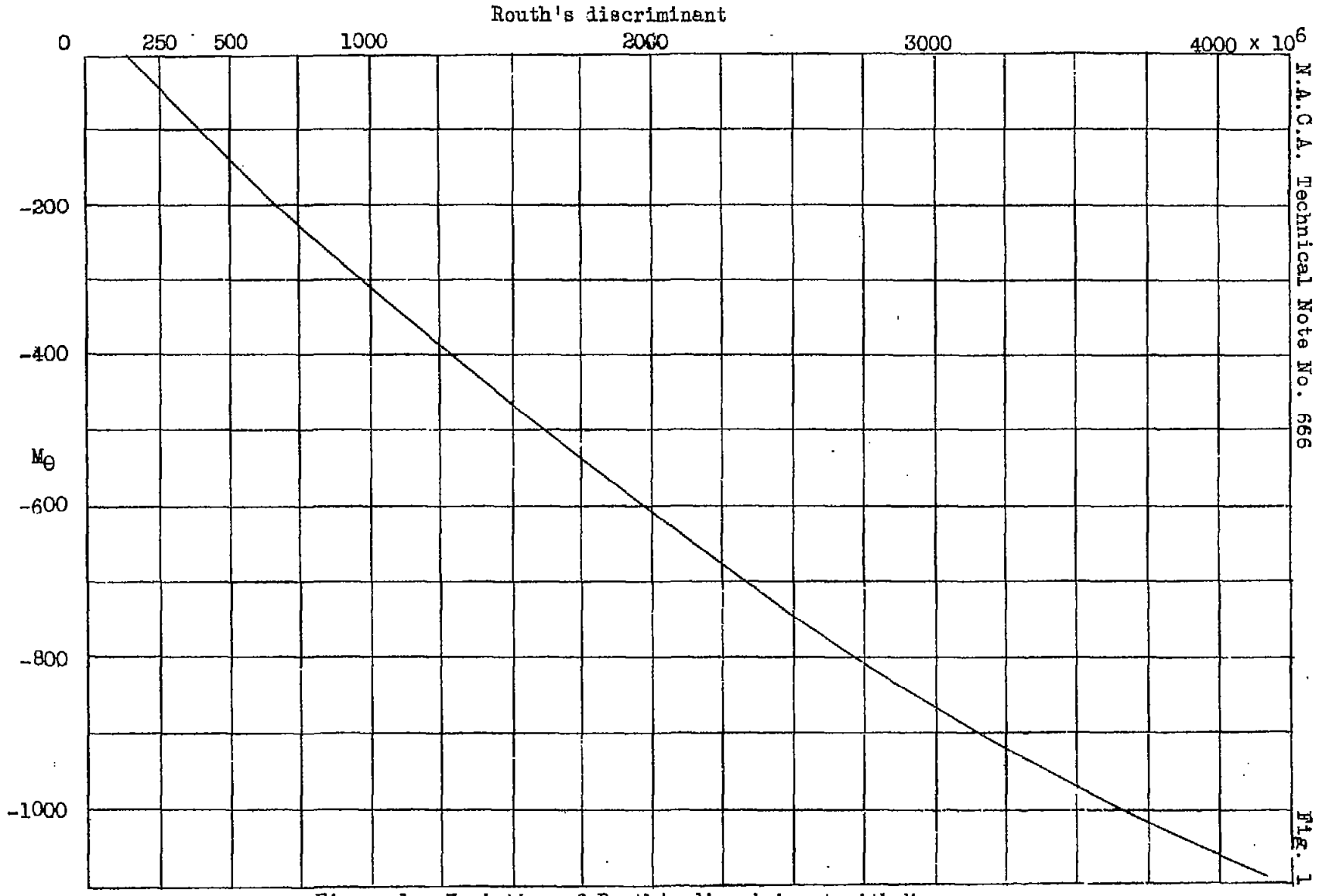

Figure 1.- Variation of Routh's discriminant with M_θ

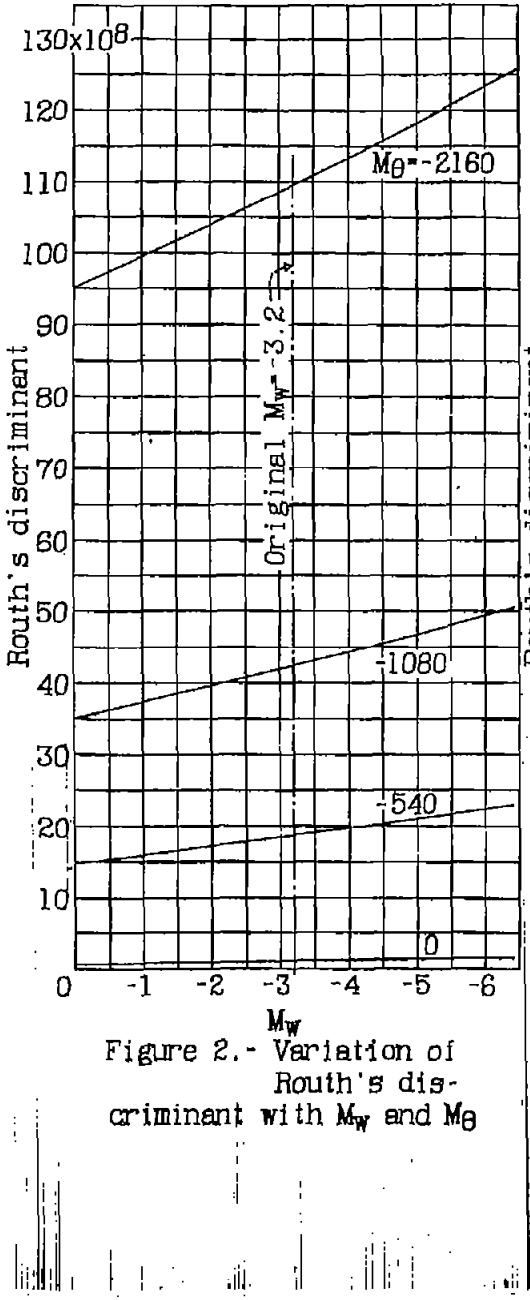

Figure 2.- Variation of Routh's discriminant with M_w and M_θ

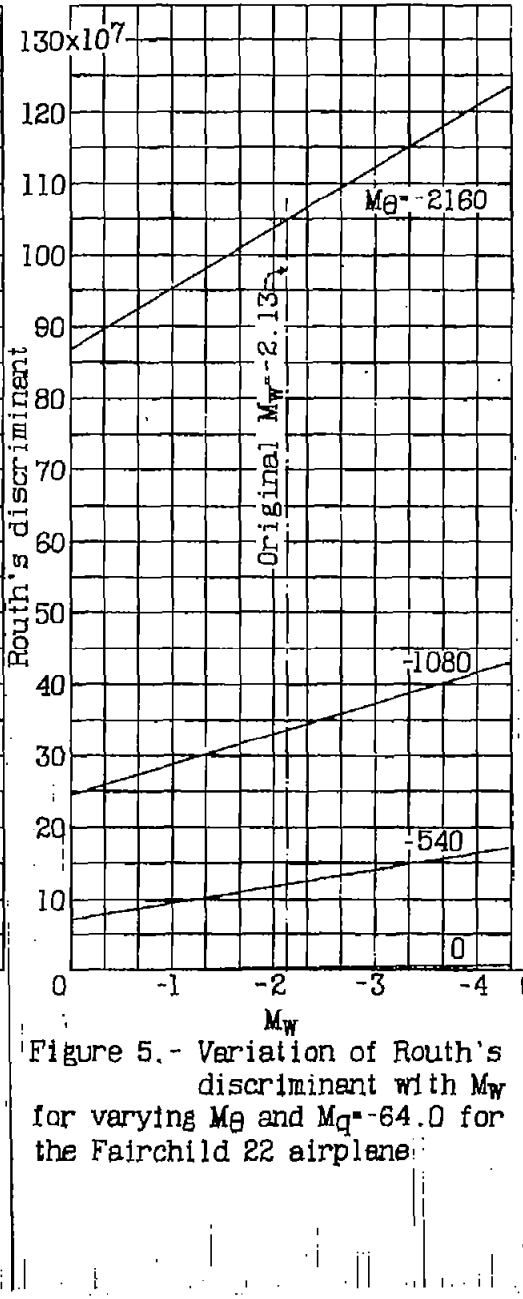

Figure 5.- Variation of Routh's discriminant with M_w for varying M_θ and M_q=-64.0 for the Fairchild 22 airplane.

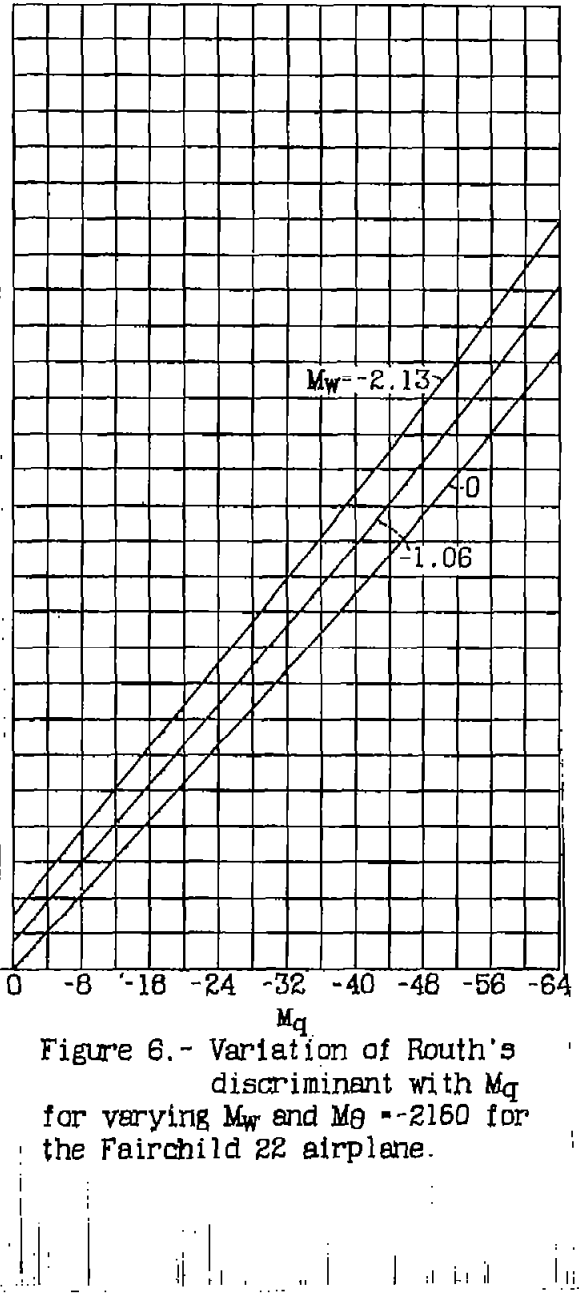

Figure 6.- Variation of Routh's discriminant with M_q for varying M_w and M_θ =-2160 for the Fairchild 22 airplane.

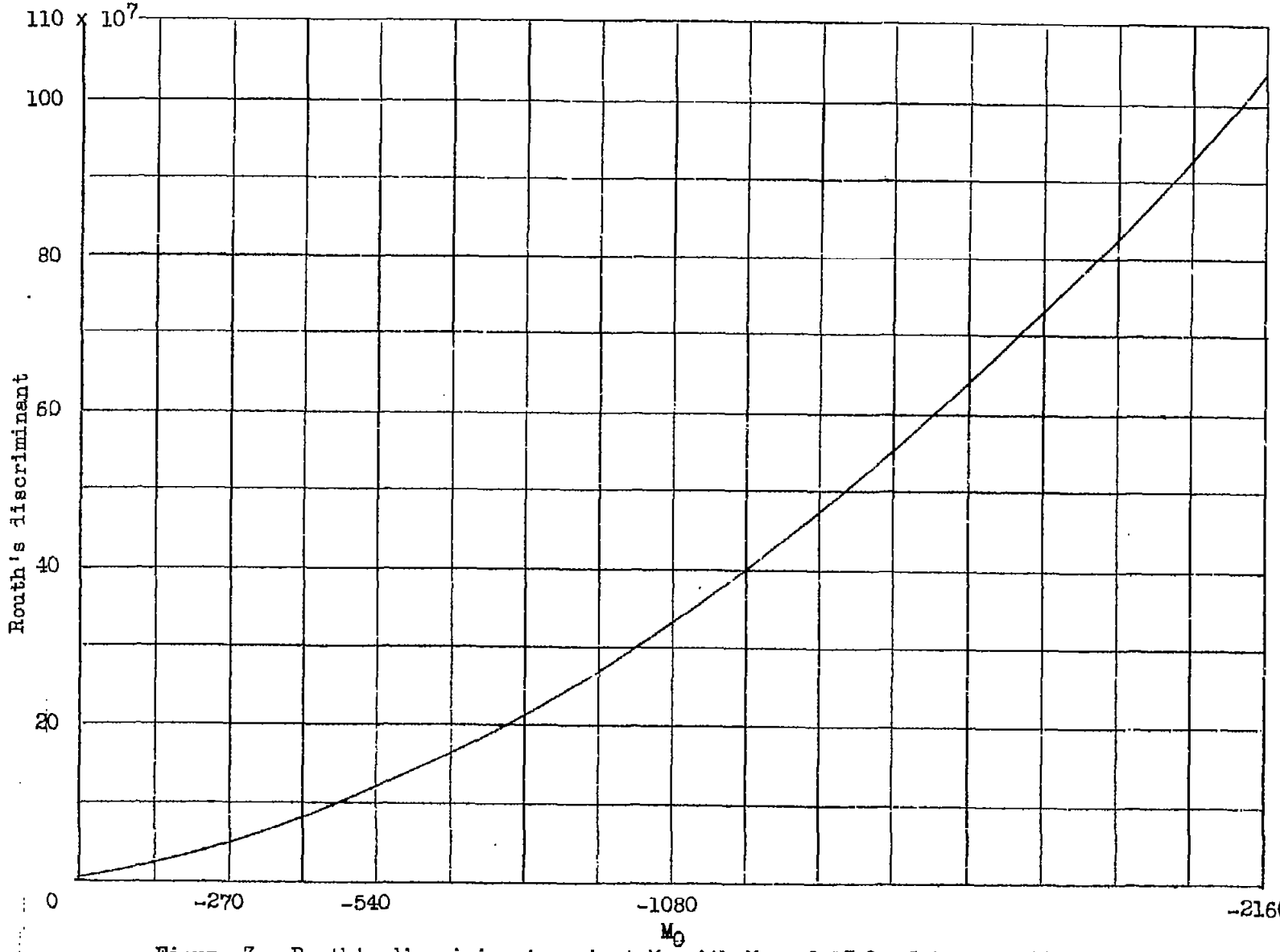

Figure 3.- Routh's discriminant against M_θ with M_w = -2.13 for Fairchild 22 airplane.

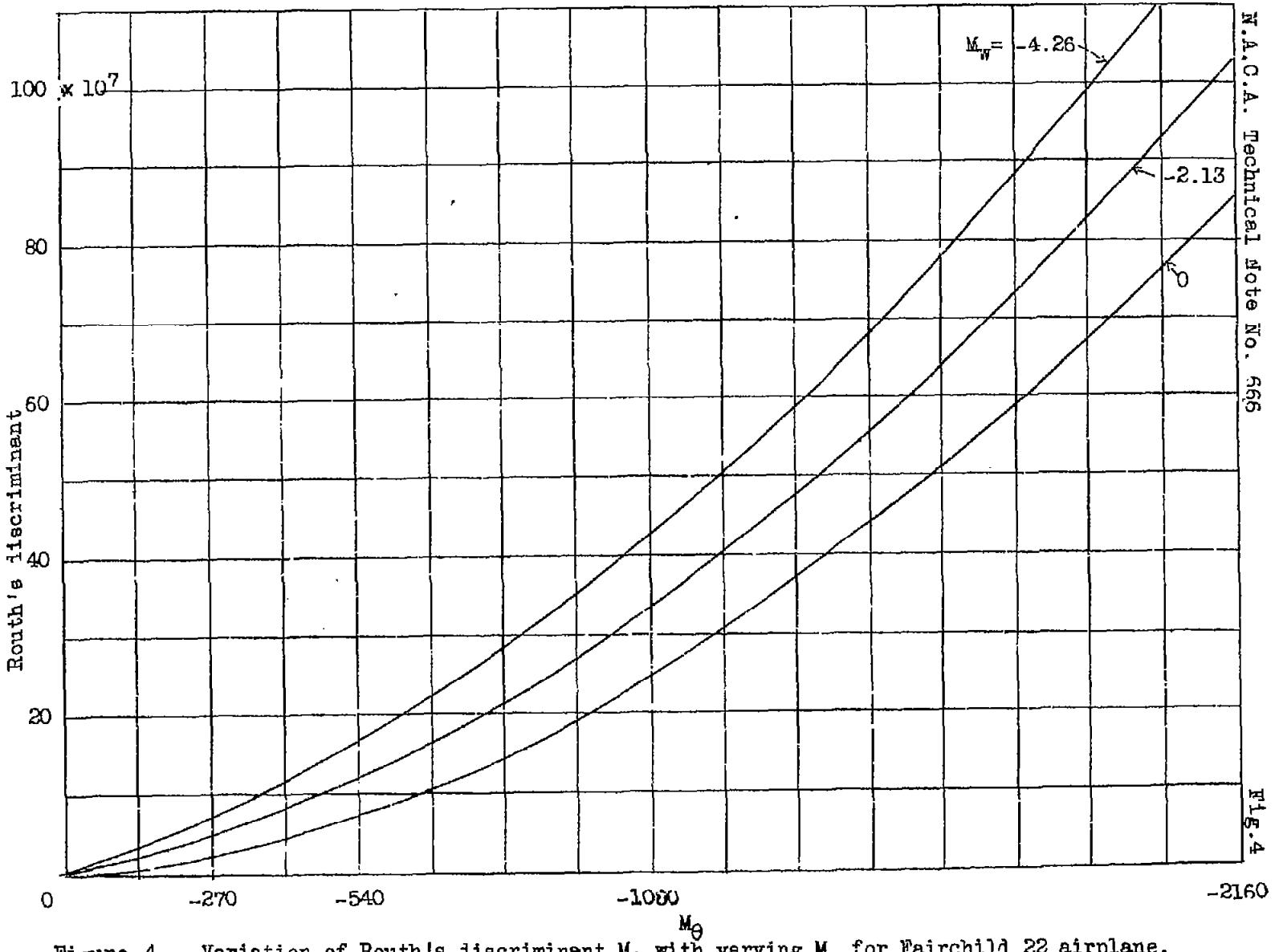

Figure 4 .-- Variation of Routh's discriminant M_θ with varying M_w for Fairchild 22 airplane.

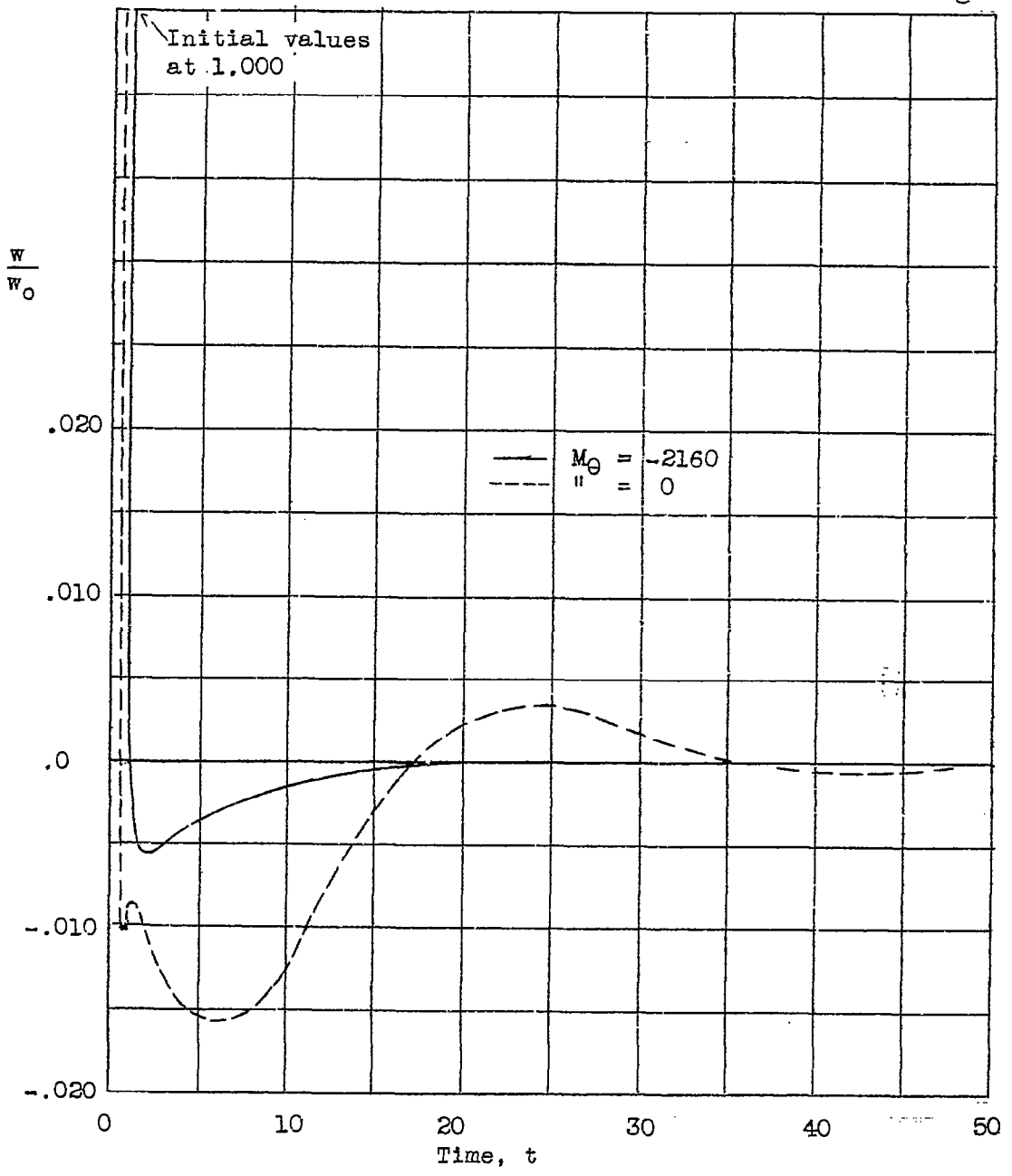

Figure 7.- Residual w/w_o against time, t for constant-velocity gust w_o.

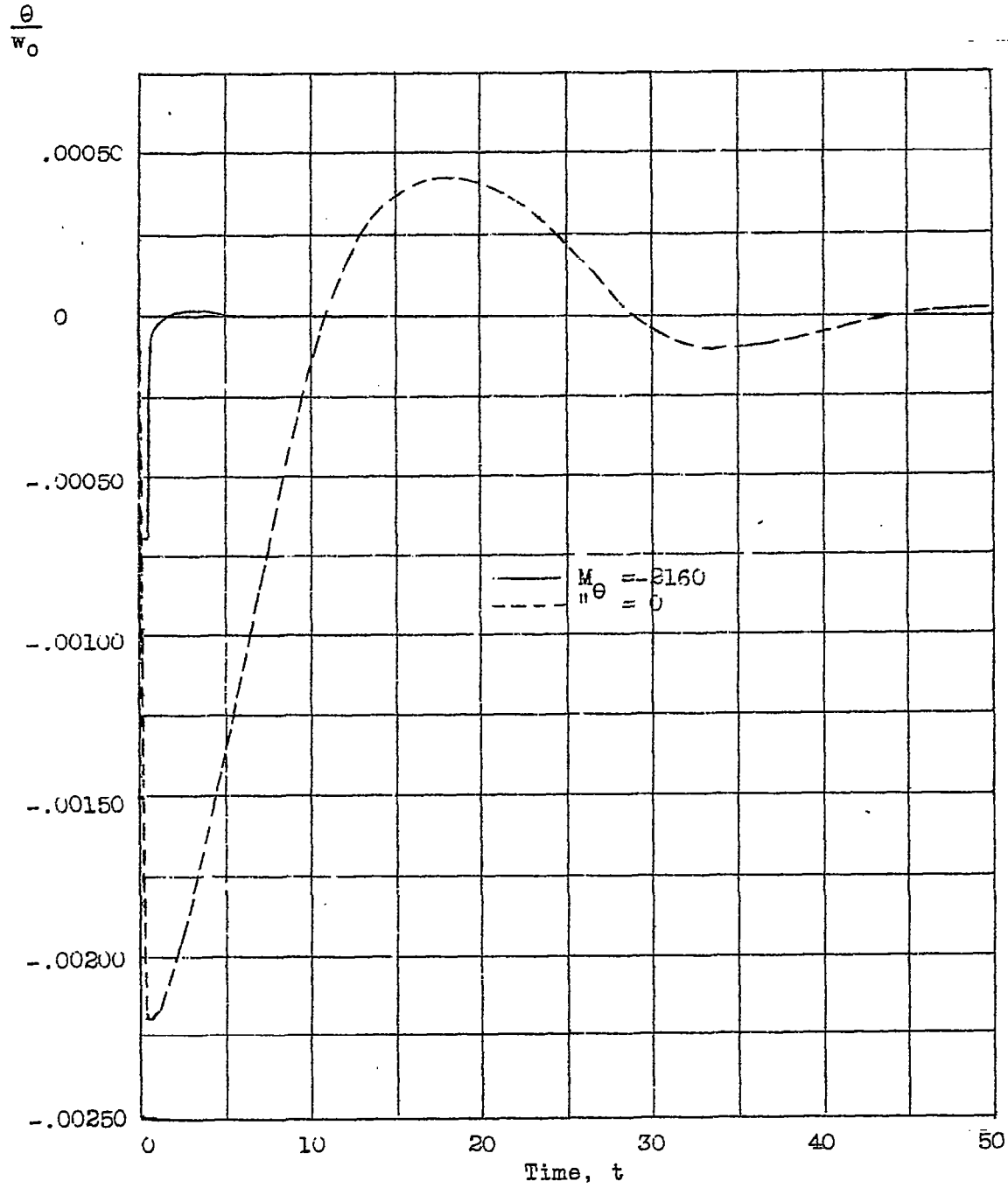

Figure 8.- Pitch angle θ against time, t for constant-velocity gust w_o.

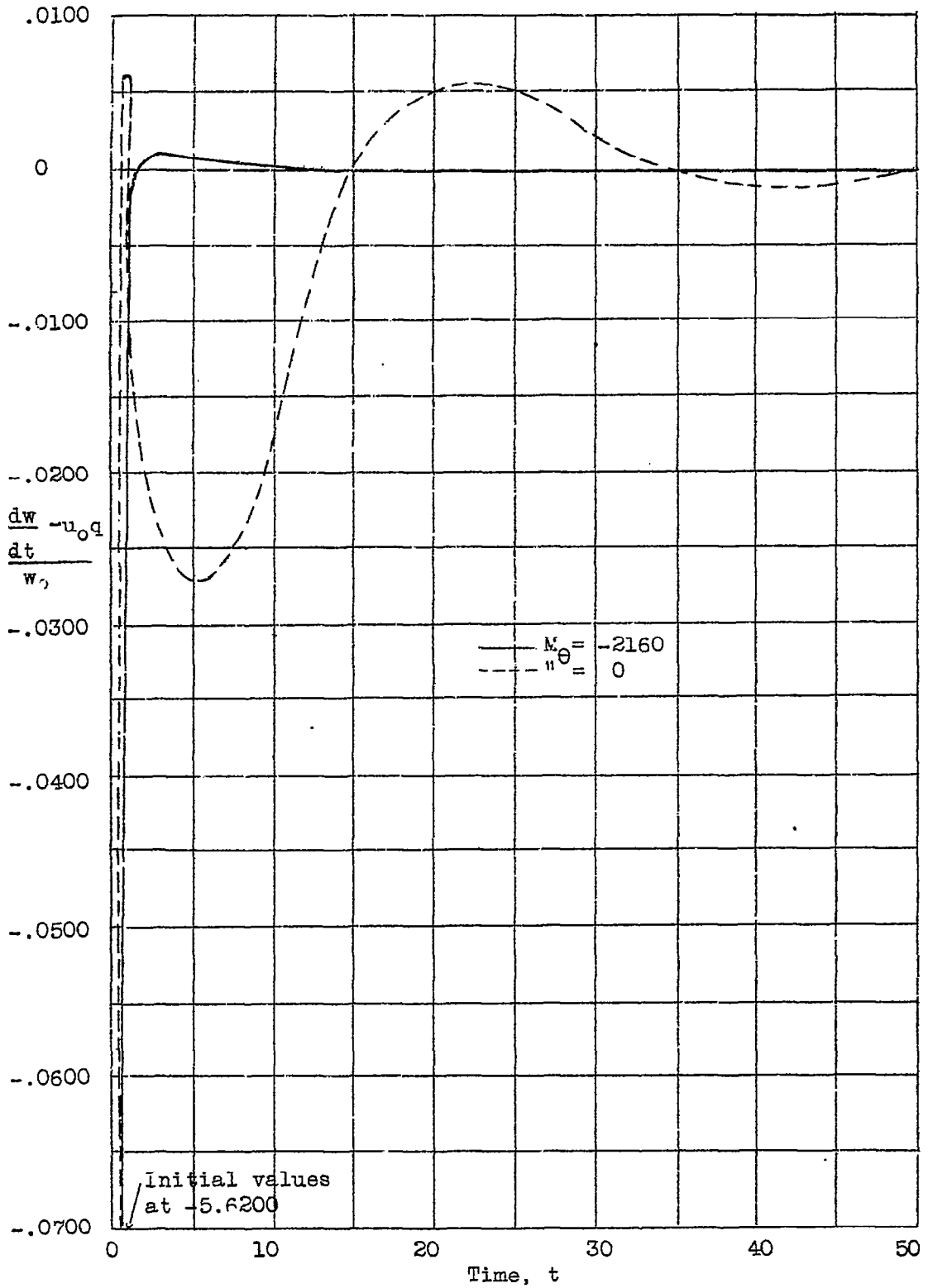

Figure 9.- $\frac{dw}{dt} - u_o q$ against time, t for constant-velocity gust w_o.

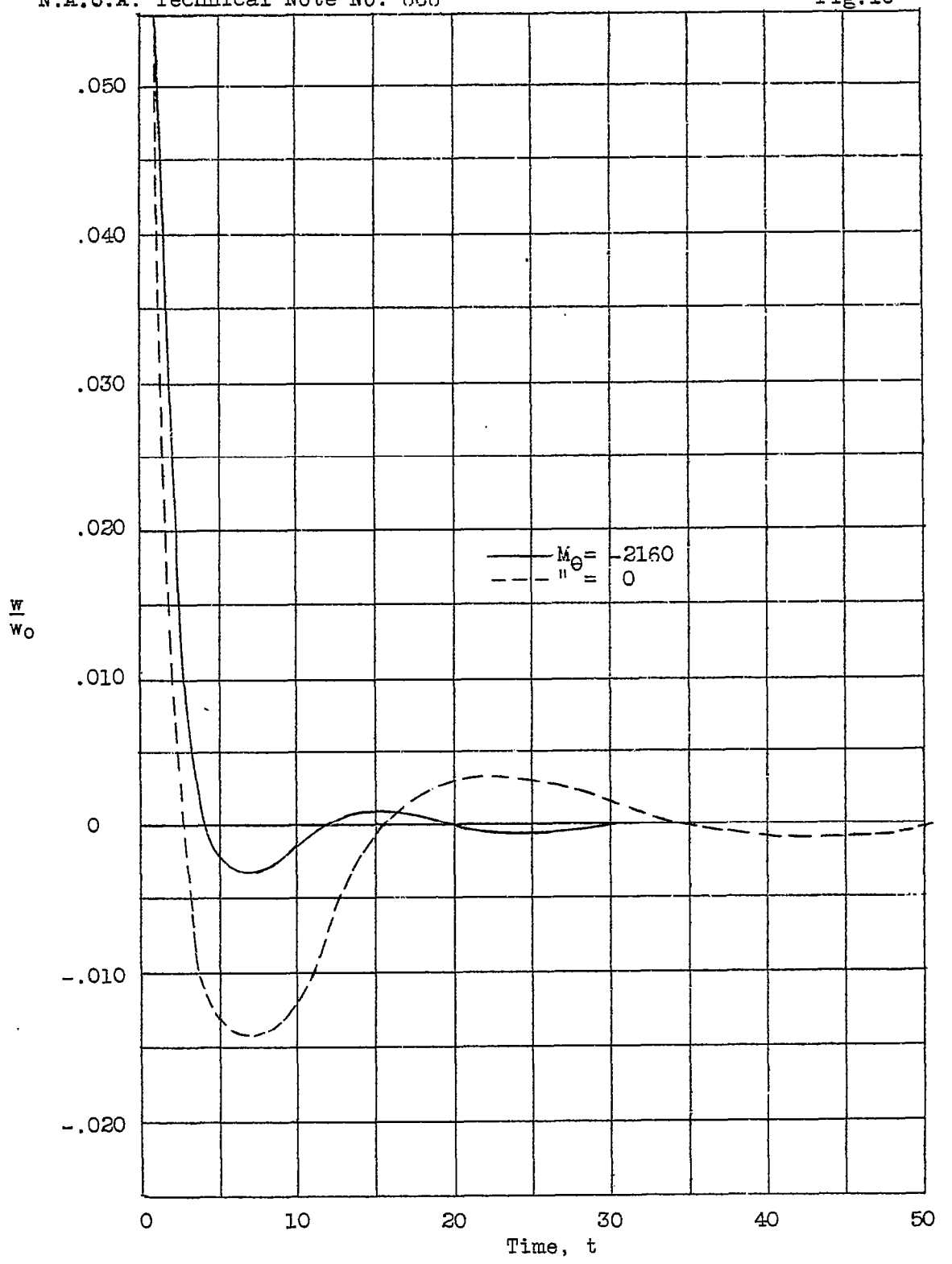

Figure 10.- Residual w against time, t for exponential gust $w_o(1-e^{-t})$.

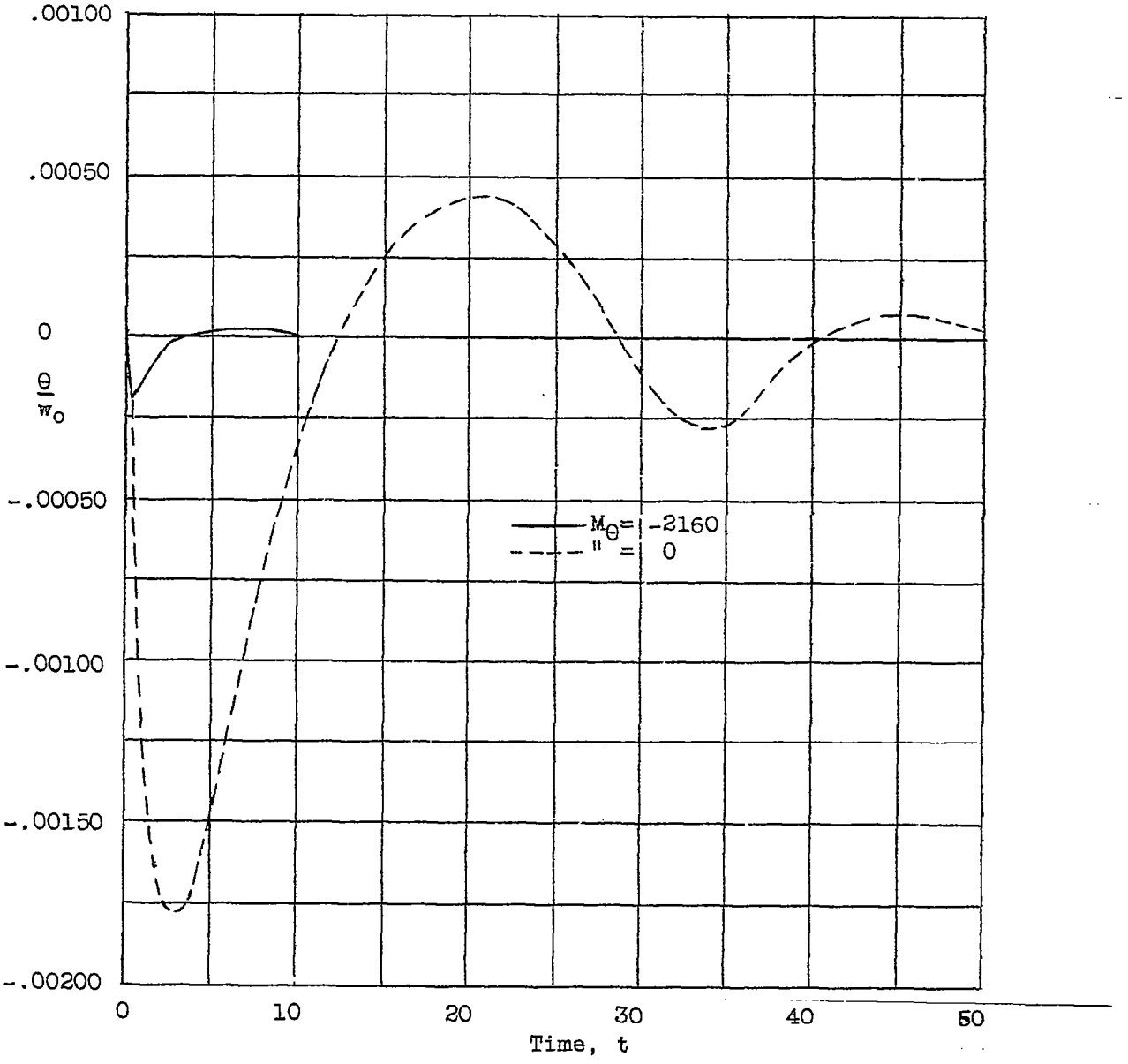

Figure.11.- Pitch angle θ against time,t for exponential gust $w_o(1-e^{-t})$.

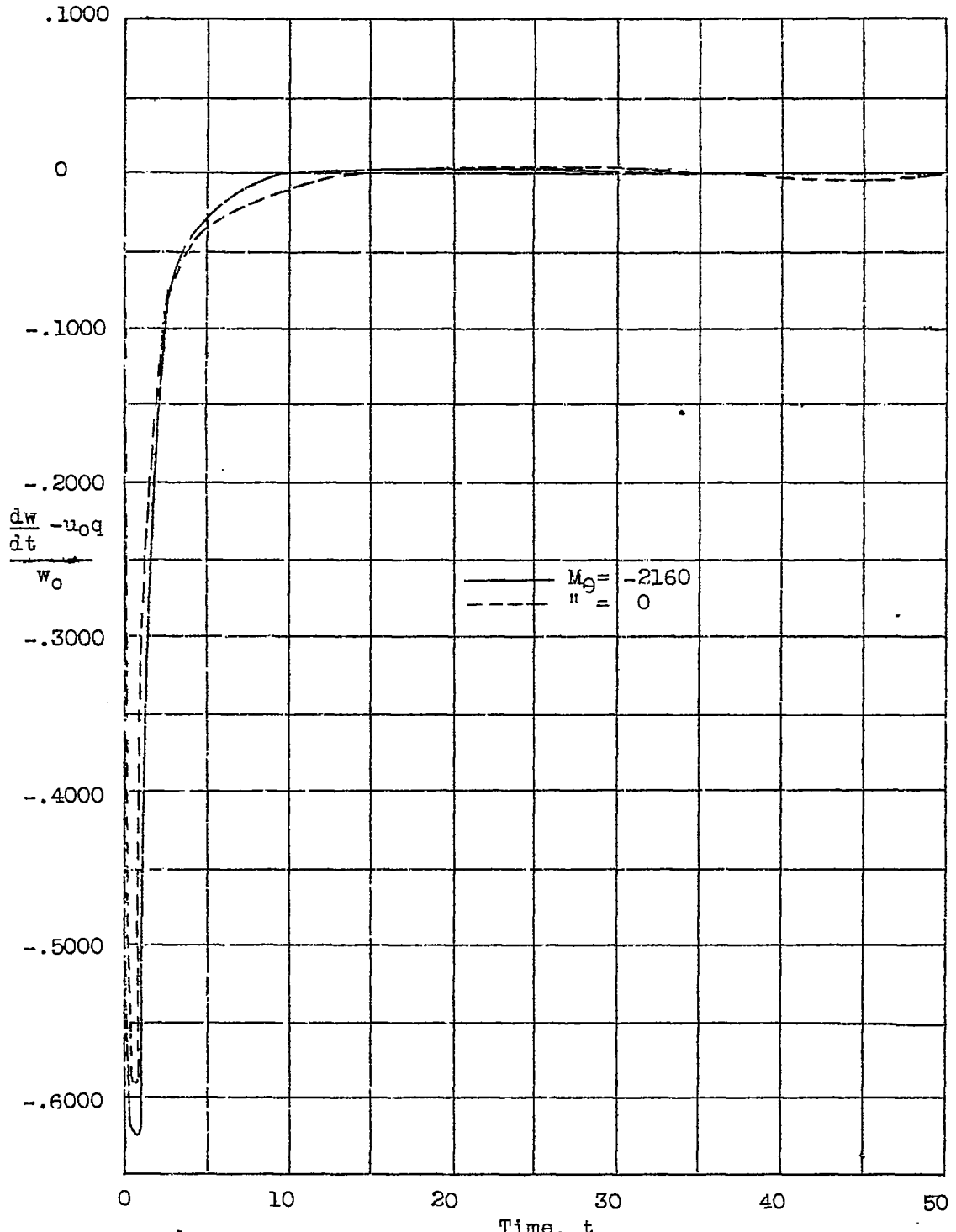

Figure12.- $\frac{dw}{it}$--$u_o q$ against time, t for exponential gust $w_o(1-e^{-t})$.

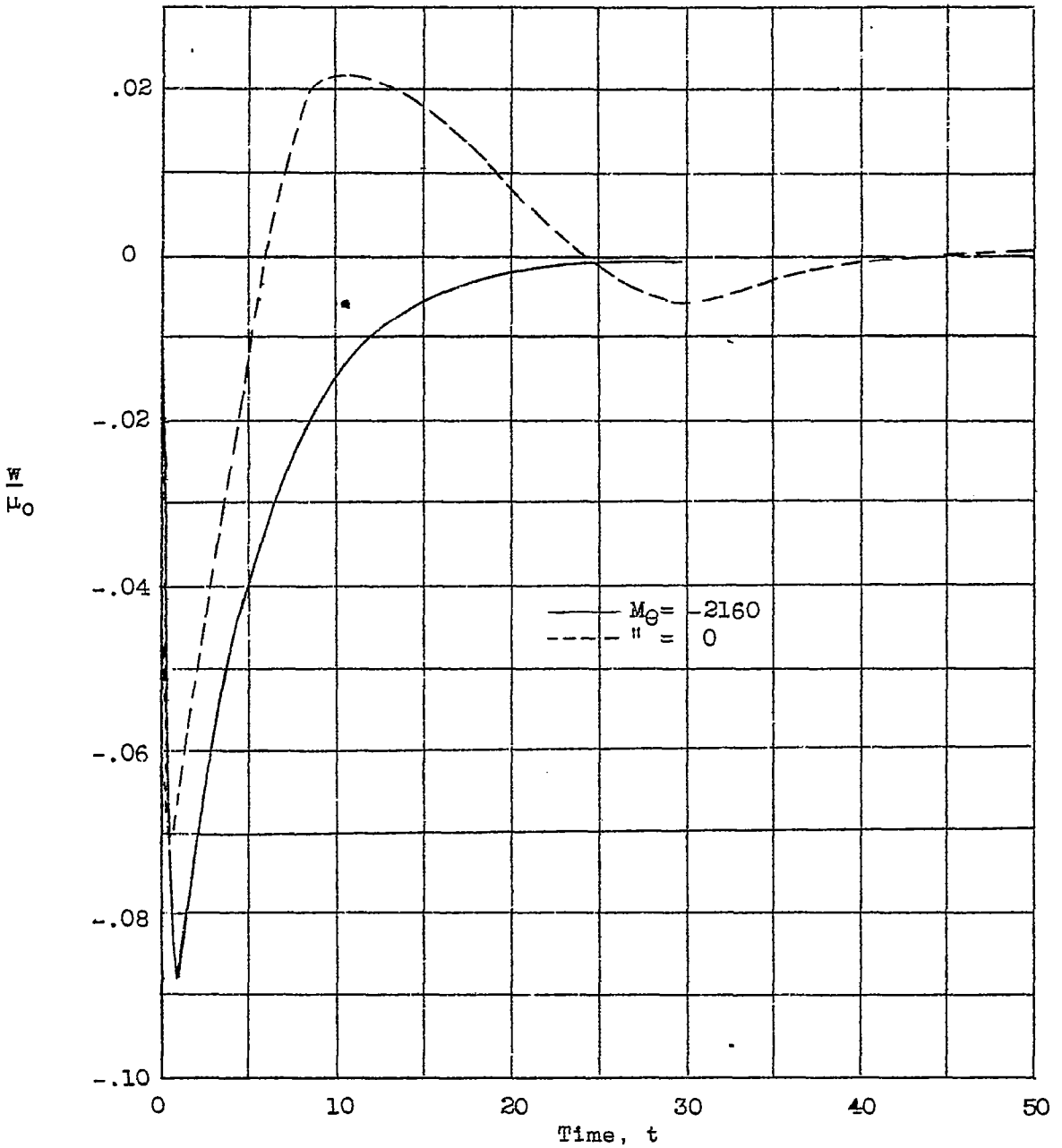

Figure 13.- Residual w against time, t for constant-velocity gust u_o.

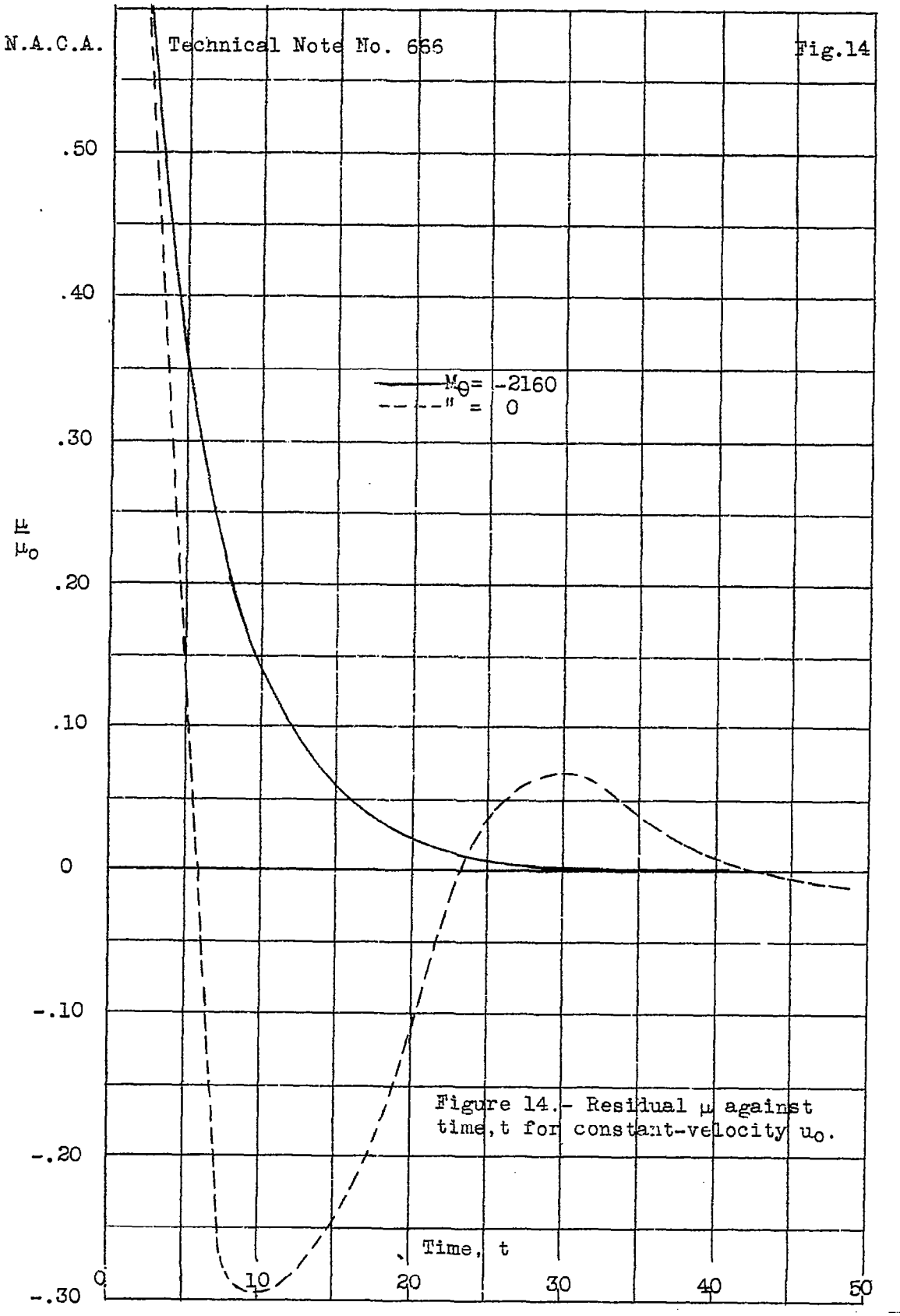

Figure 14.- Residual μ against time, t for constant-velocity u_0.

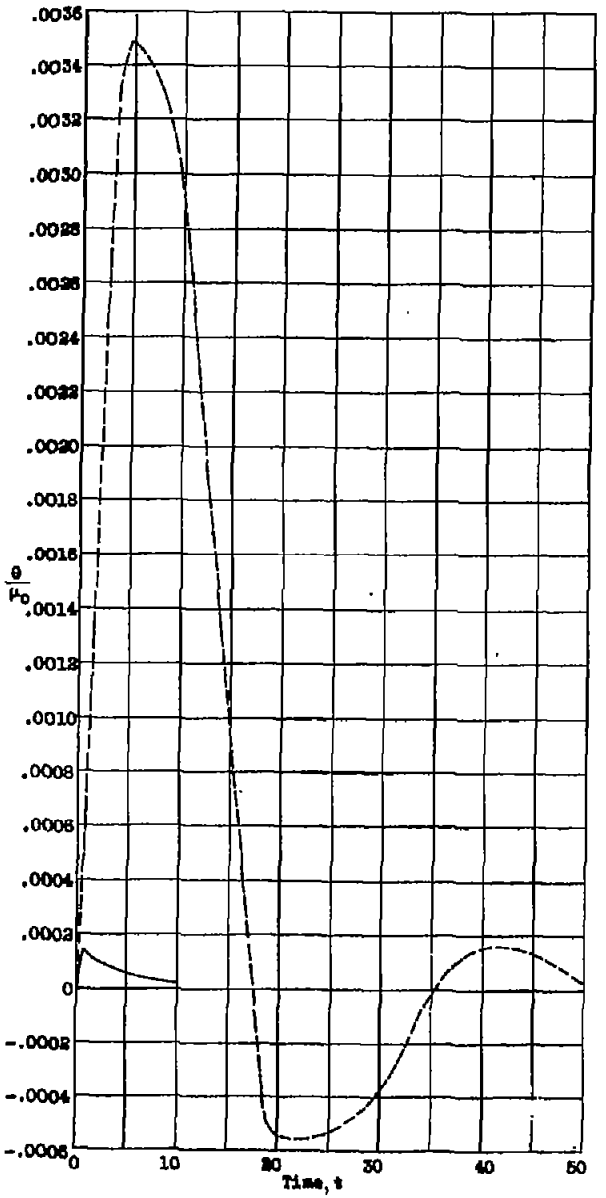

Figure 15.- Pitch angle θ against time t for constant velocity gust u_o

——— M_θ=-2160

- - - - M_θ= 0.

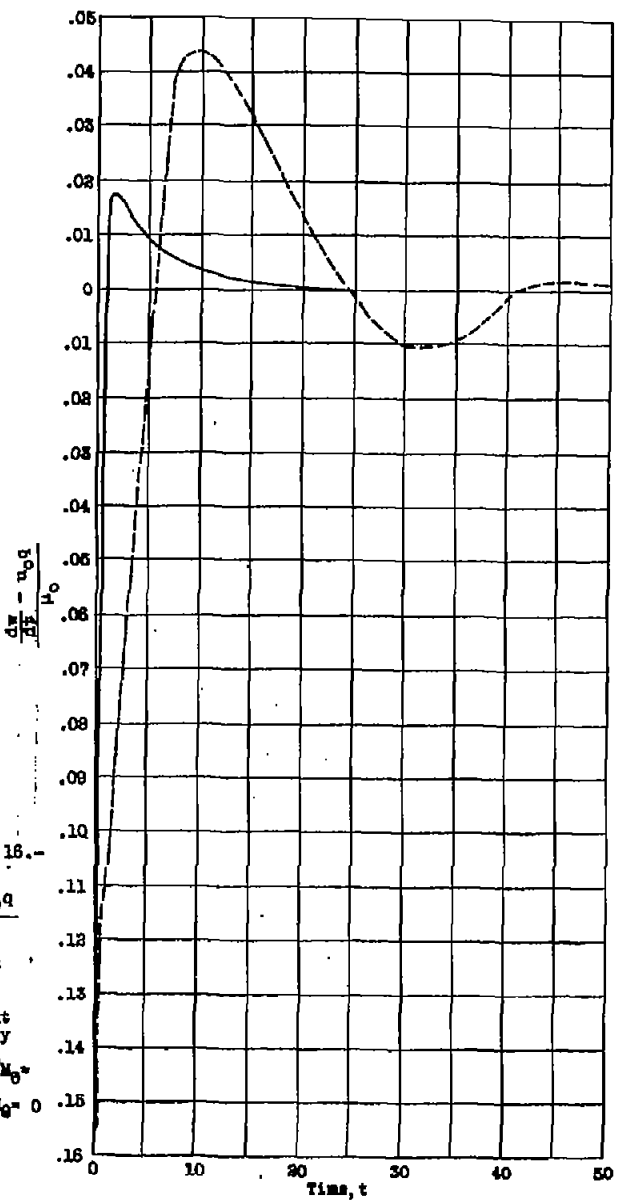

Figure 16.- $\frac{\frac{dw}{dt} - u_o q}{\mu_o}$ against time t for constant velocity gust u_o

——— M_θ= -2160

- - - - M_θ= 0

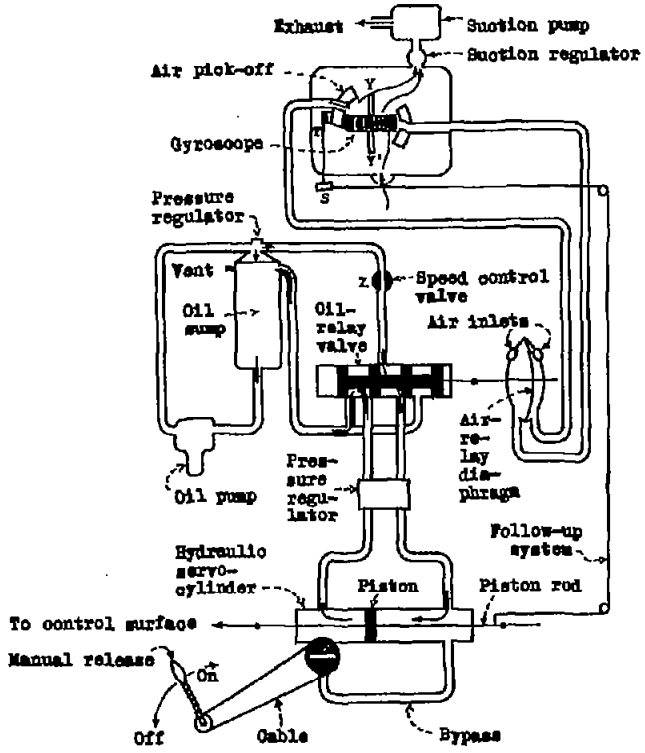

Figure 17. - Schematic diagram of elevator control of Sperry Gyropilot, (figure 11 of reference 3)

A. Motion due to the lag moment, $-M_{\theta}\theta_g$
B. Motion due to gust and lag moment, $-M_{\theta}\theta_g$
C. Motion due to reversed-lag moment, $+M_{\theta}\theta_g$
D. Superposition of B and C (with C displaced by 0.25 sec).

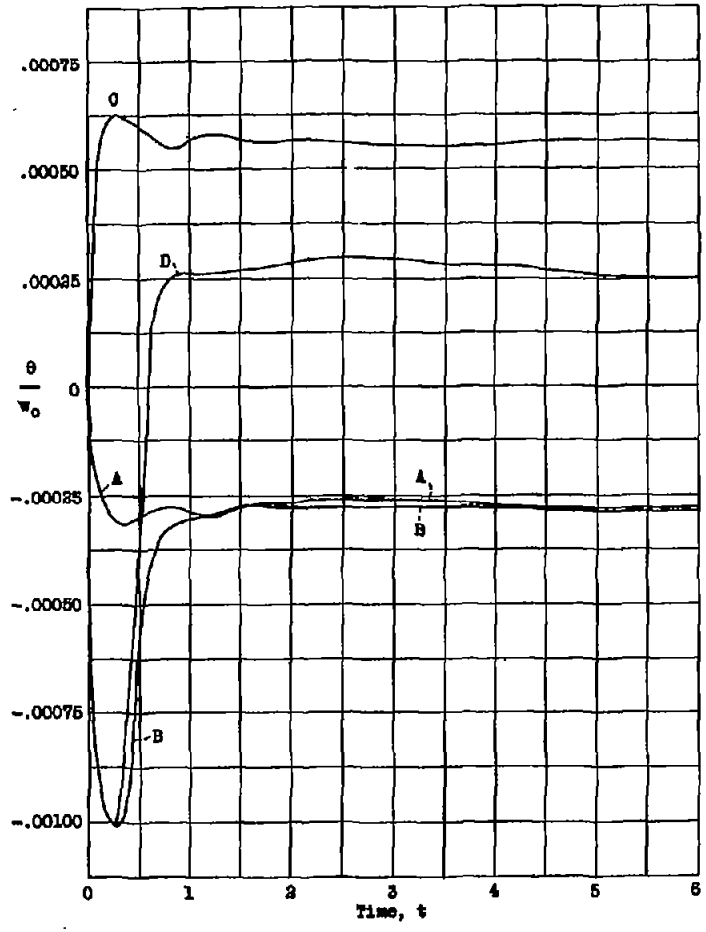

Figure 20. - Solution for θ/w_o.

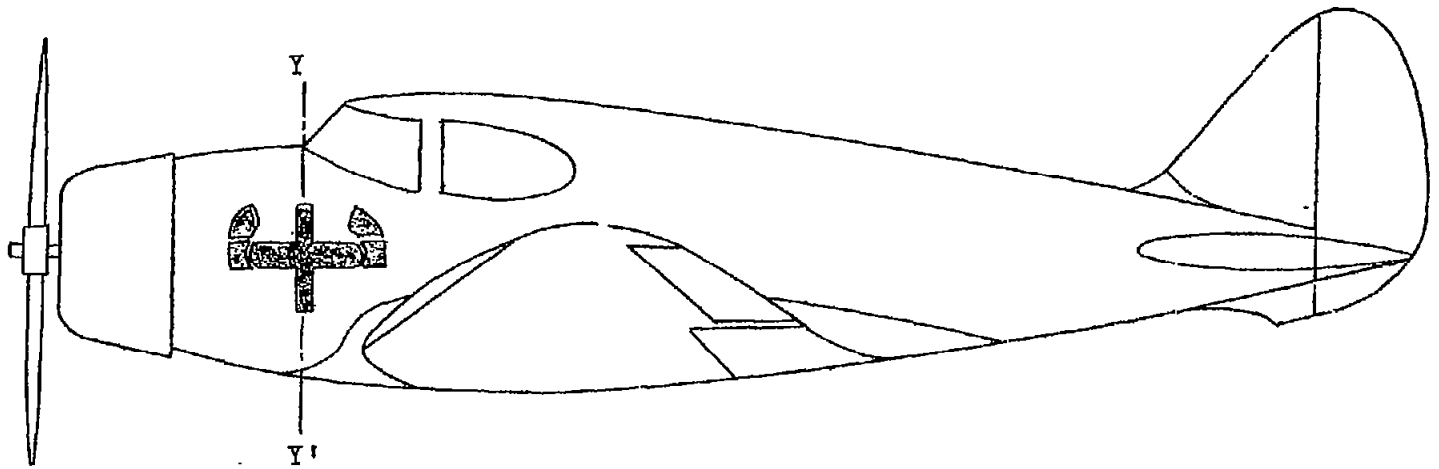

Figure 18.- Airplane flying on level keel.

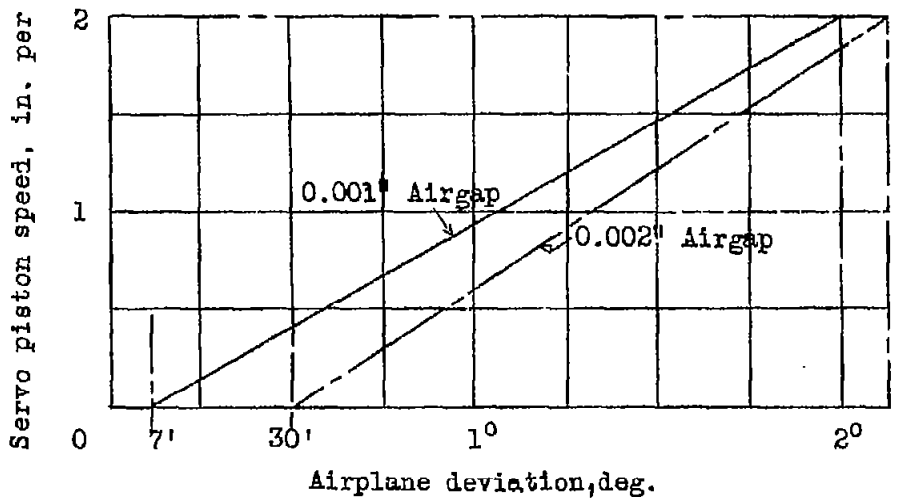

Figure 19.- Variation of servo-piston speed with airplane deviation.

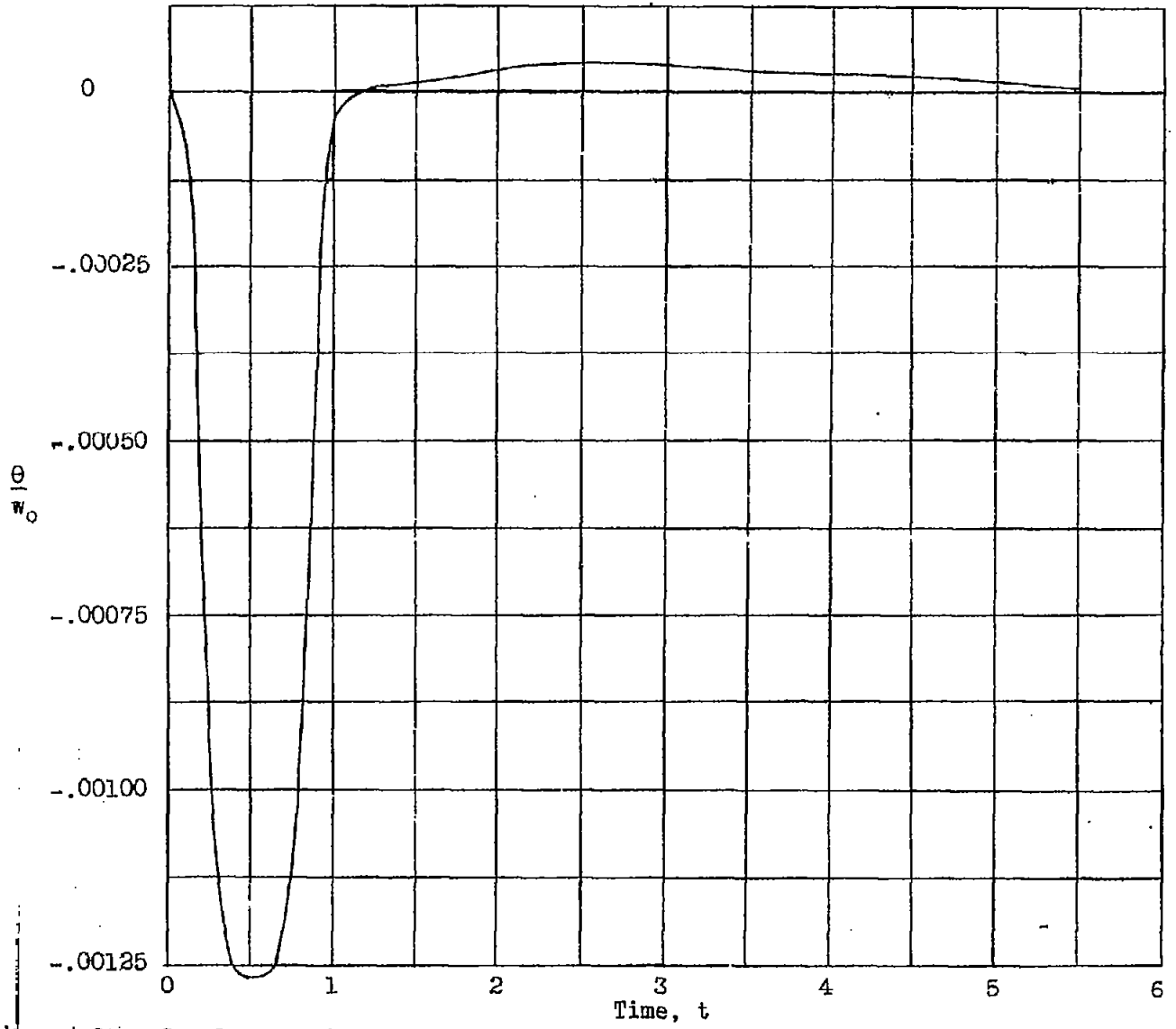

Figure 21.- Complete motion under a vertical gust in pitch with automatic pilot lag taken into account.

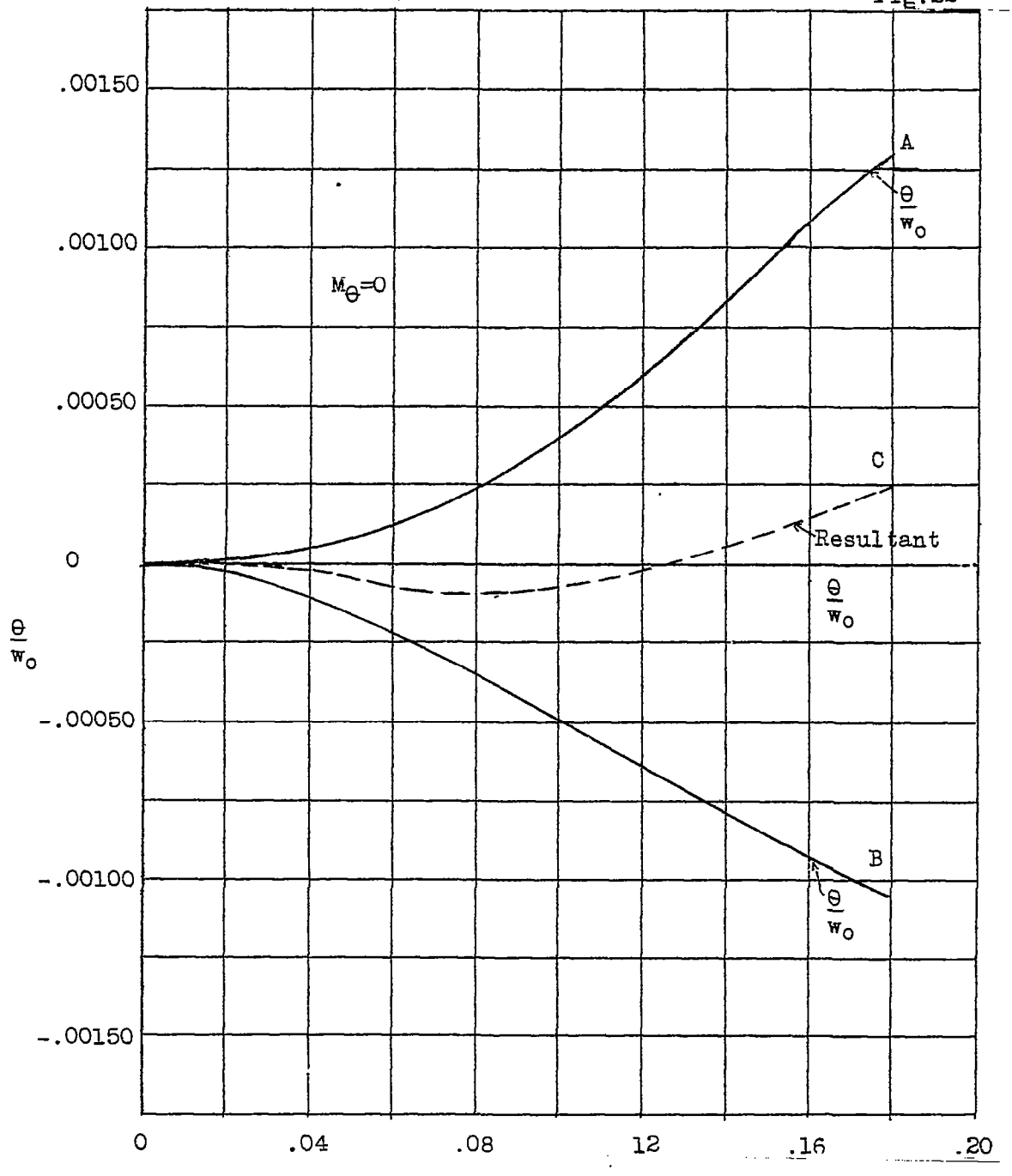

Figure 22.- Solution of equation (VIII-3) for $M_\theta=0$.

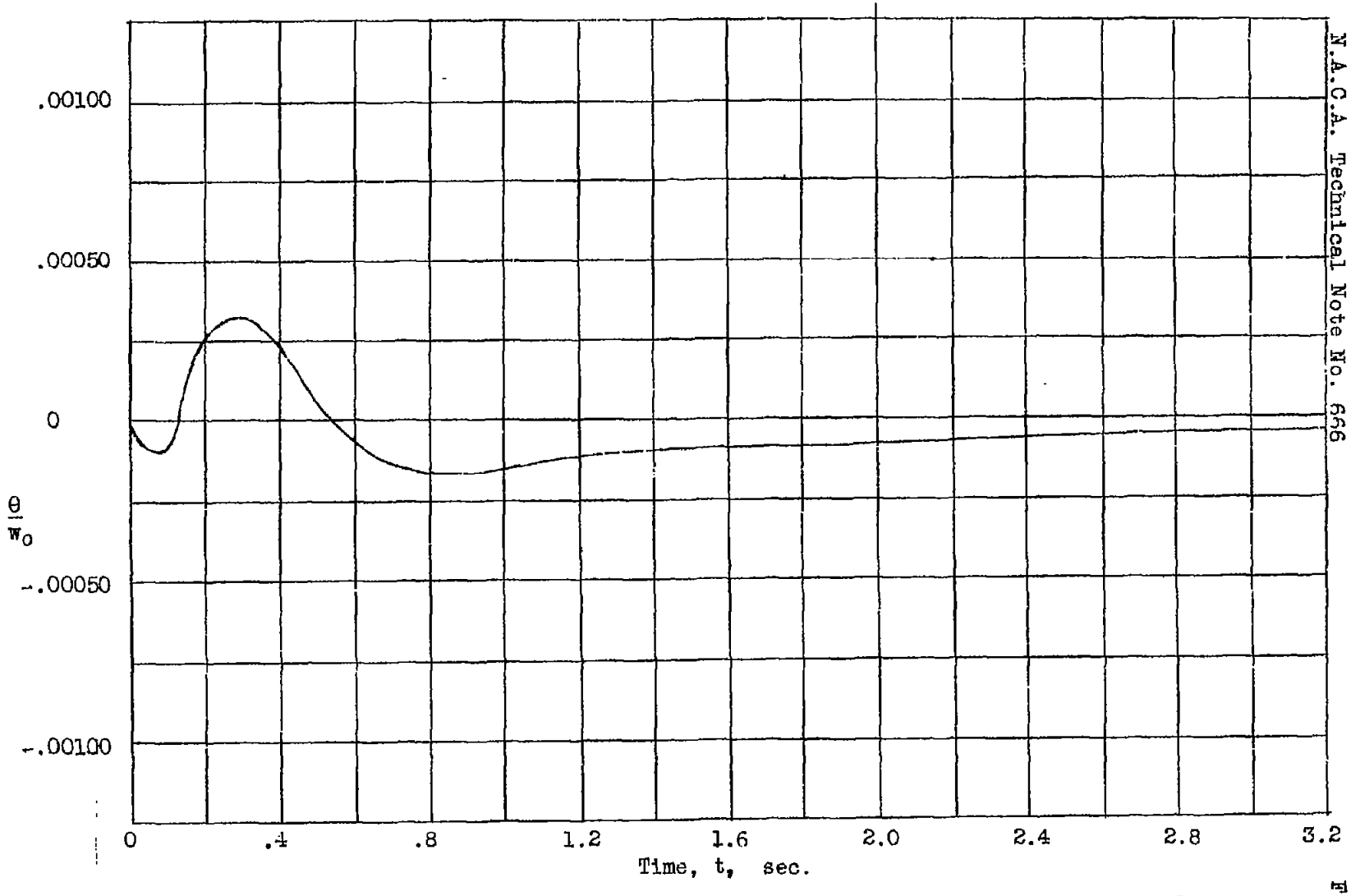

Figure 23.- Complete motion in pitch of the Clark biplane upon entering a vertical gust.